SAND2016-9603PE

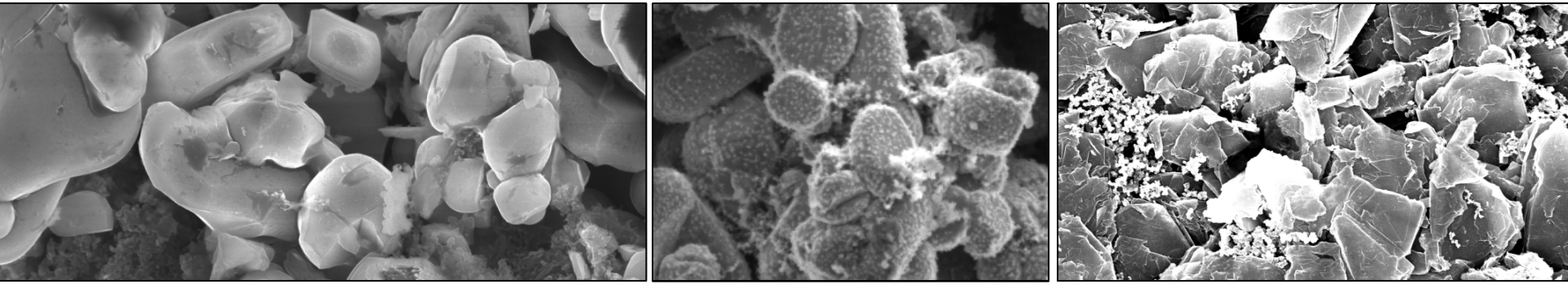

The Effects of Cycle Rate on Capacity Fade of Lithium Ion Batteries

Chelsea Snyder

PhD Graduate Student

Sandia National Laboratories is a multi-program laboratory managed and operated by Sandia Corporation, a wholly owned subsidiary of Lockheed Martin Corporation, for the U.S. Department of Energy's National Nuclear Security Administration under contract DE-AC04-94AL85000.

Rensselaer

Sandia National Laboratories

Motivation

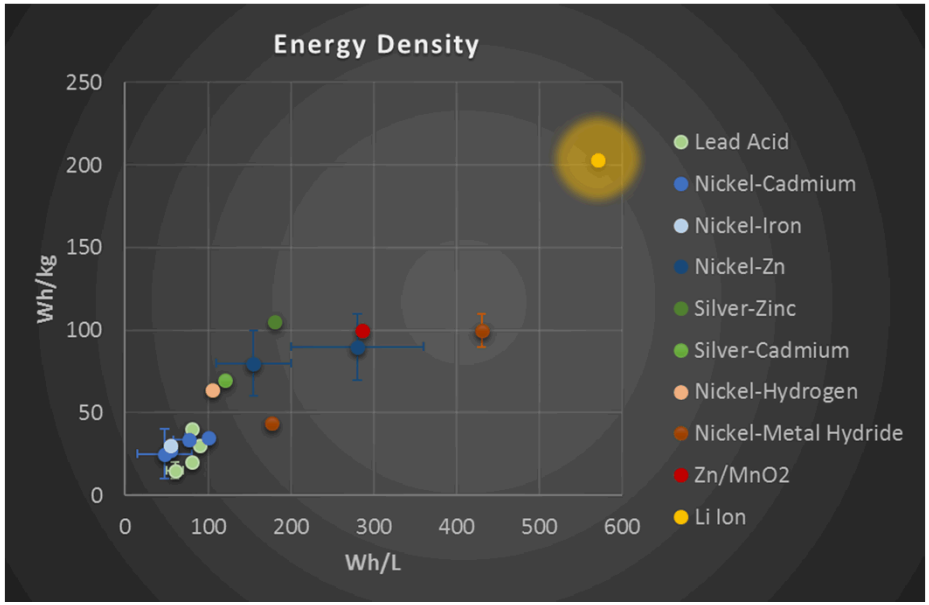

Data from Linden, D., *Linden's Handbook of Batteries*. Fourth ed. 2011: The McGraw-Hill Companies, Inc.

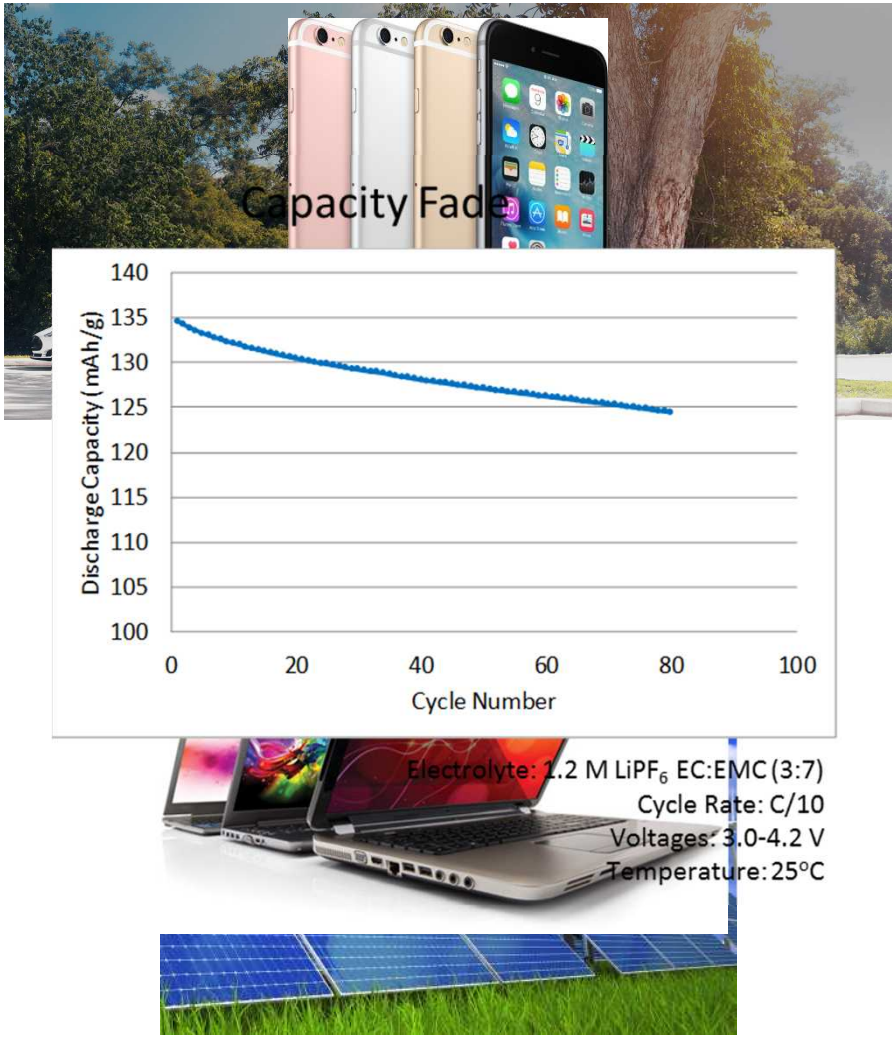

C-rate Effects

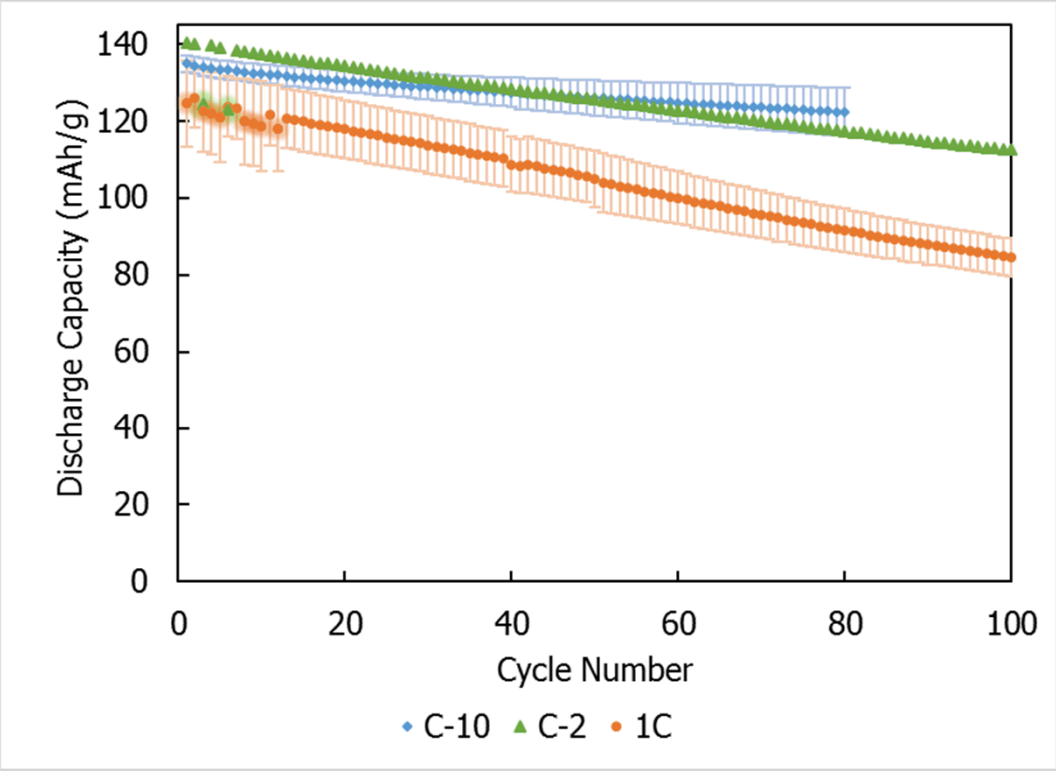

Electrolyte: 1.2M $LiPF_6$ EC:EMC (3:7)
Voltage: 3.0 to 4.2V CCCV
Temperature: 25°C

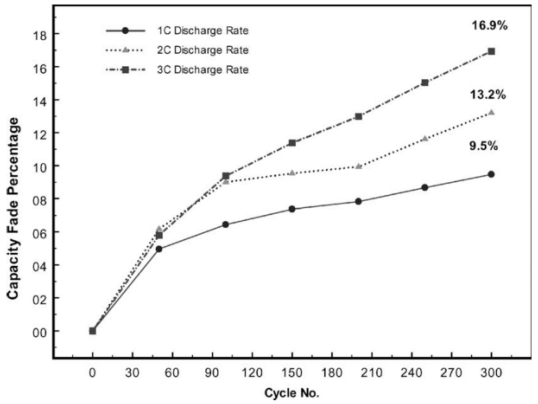

G. Ning, B. Haran, B. Popov *J. Power Sources* 117 (2003) 160-169

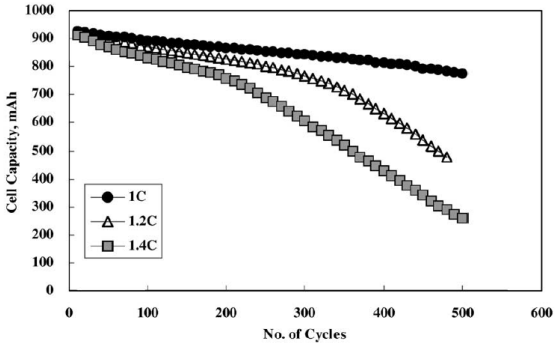

C. Soo Seok and H. S. Lim *J. Power Sources* 111 (2002) 130-136

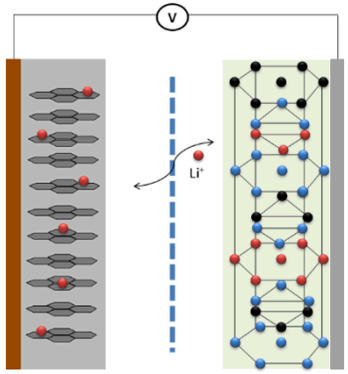

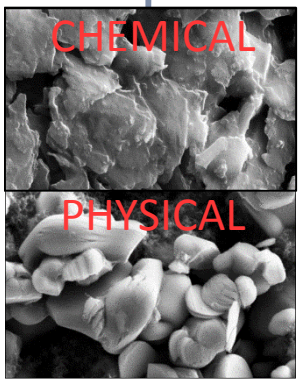

THESIS HYPOTHESIS

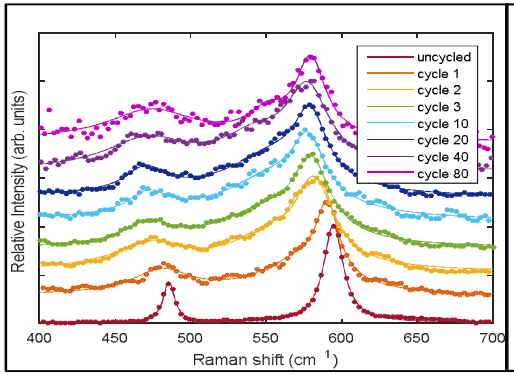

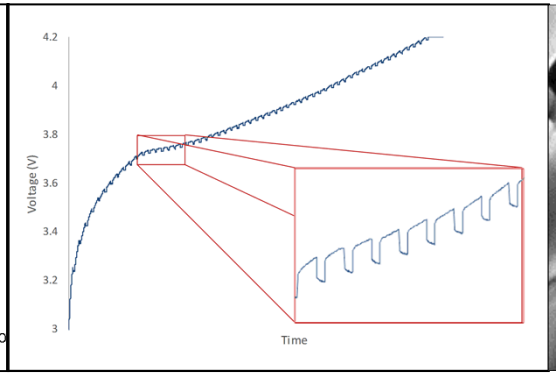

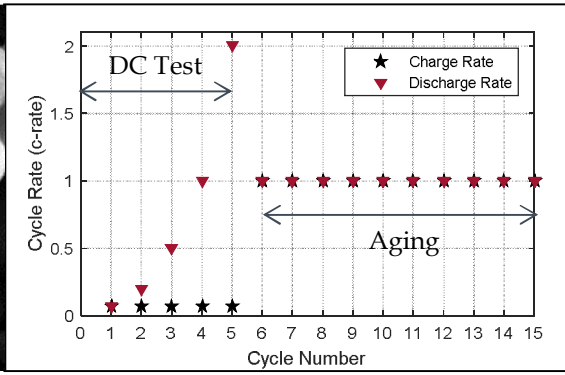

RAMAN SPECTROSCOPY CURRENT INTERRUPT MICROSCOPY RATE CAPABILITY

Batteries

- A battery converts stored chemical energy into electrical energy through an electrochemical oxidation-reduction reaction
- Anode: oxidized species
- Cathode: reduced species

"Rocking Chair"

$$LiCoO_2 + \frac{x}{y}C \underset{discharge}{\overset{charge}{\rightleftharpoons}} \frac{x}{y}Li_yC + Li_{1-x}CoO_2$$

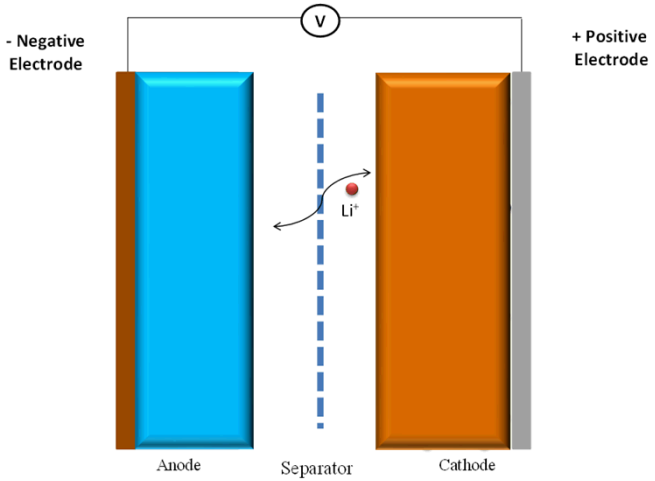

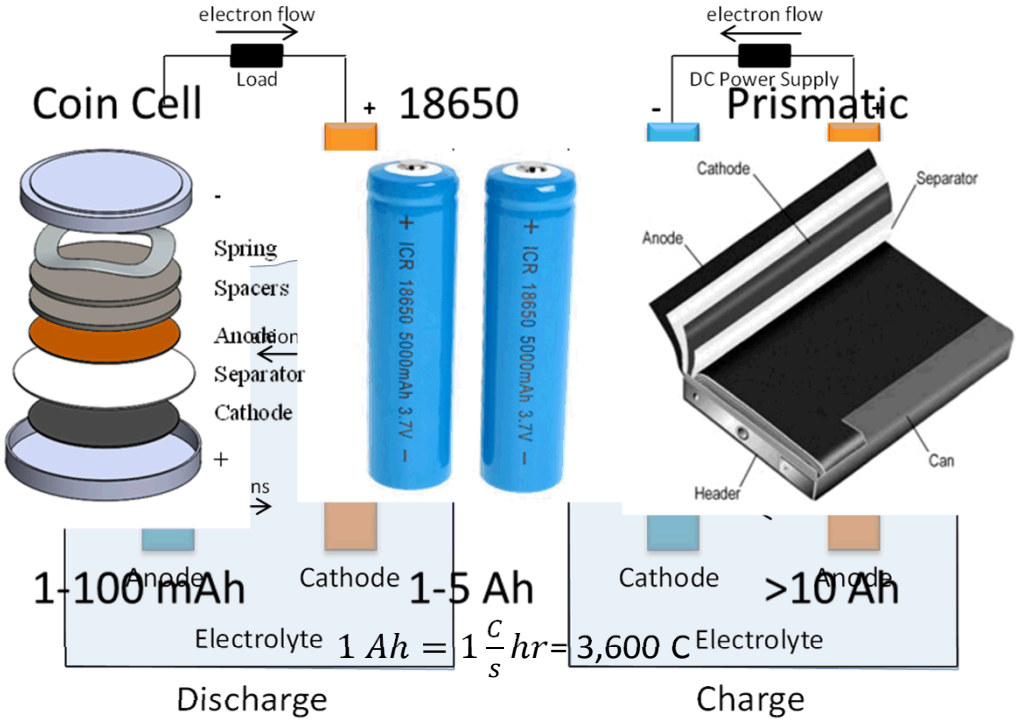

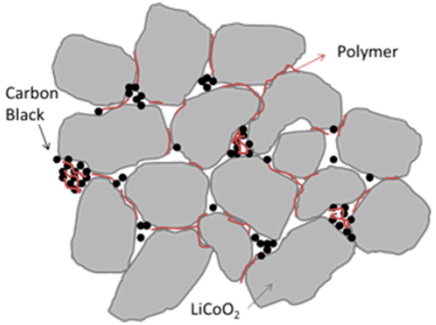

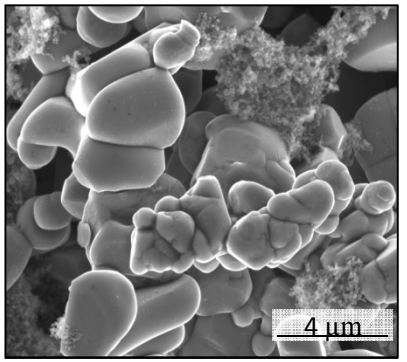

Linden, D., *Linden's Handbook of Batteries*. Fourth ed. 2011: The McGraw-Hill Companies, Inc.
J. Goodenough and K. Park *Journal of American Chemical Society* 135 (2013) 1167-1176

LIB TECHNOLOGY

DEGRADATION

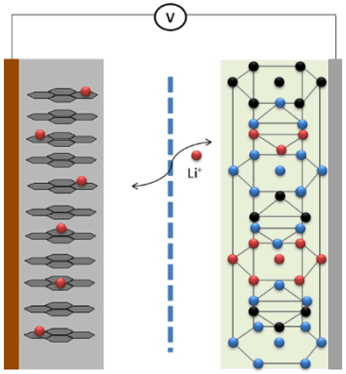

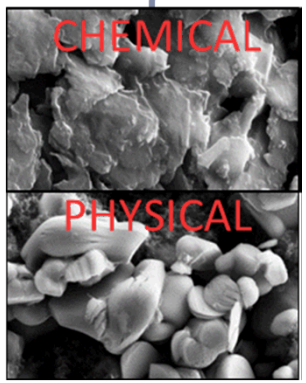

Graphitic Electrode

1. Solid Electrolyte Interphase (SEI) formation
   - Reduction of electrolyte to form passive surface film
   - Largest impact during first few cycles
   - Grows with square root time
2. Lithium plating
   - Li dendrite formation
   - Caused by high polarization of graphitic electrode (poor kinetics)
3. Structural disorder and damage
   - 10% linear expansion at full charge
4. Contact loss in composite material due to expansion of graphite

$$L = \sqrt{Dt}$$

L: Characteristic Length
D: Diffusion coefficient
t: time

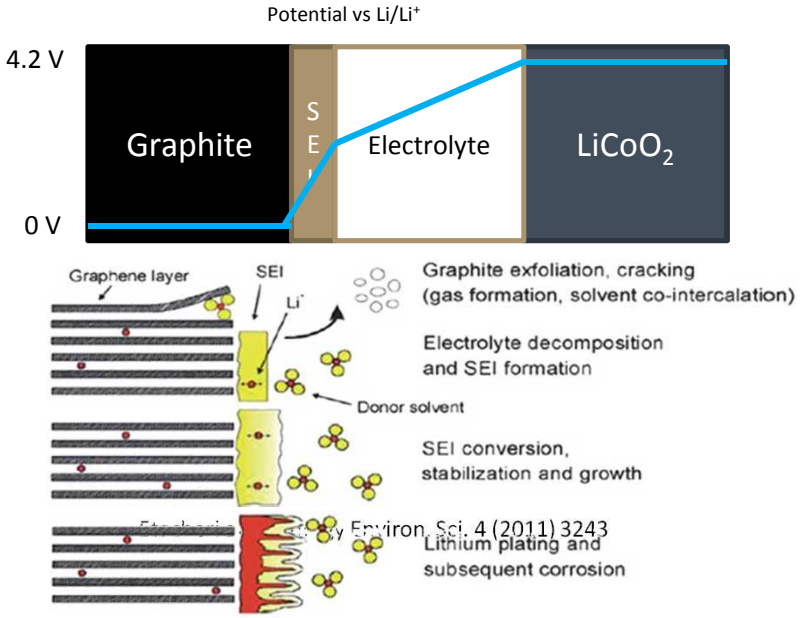

Etacheri et al. Energy Environ. Sci. 4 (2011) 3243

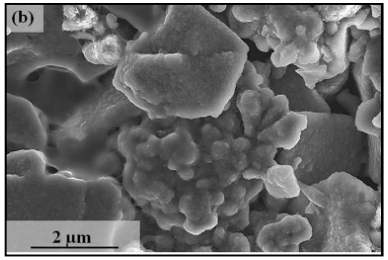

J. Lee et al. *Carbon* 52 (2013) 388-397

Mukhopadhyay, A., et al *Electrochimica Acta* 66 (2012) 28-37
Y. Koyama et al *Advanced Functional Materials* 16 (2006) 492-498
Shengshui, Z., et al *Electrochemical and Solid-State Letters* 4 (2001) A206-A208
Matsumura, Y., S. Wang, and J. Mondori *Journal of the Electrochemical Society* 142 (1995) 2914-2918

$LiCoO_2$ Electrode

1. Anisotropic expansion/contraction
   - Internal strains and dislocation defects
   - Fracture of particles
2. Electrode disordering
   - Deactivation of Li ions
   - Triggered by strain caused by volumetric changes
3. Electrolyte Oxidation

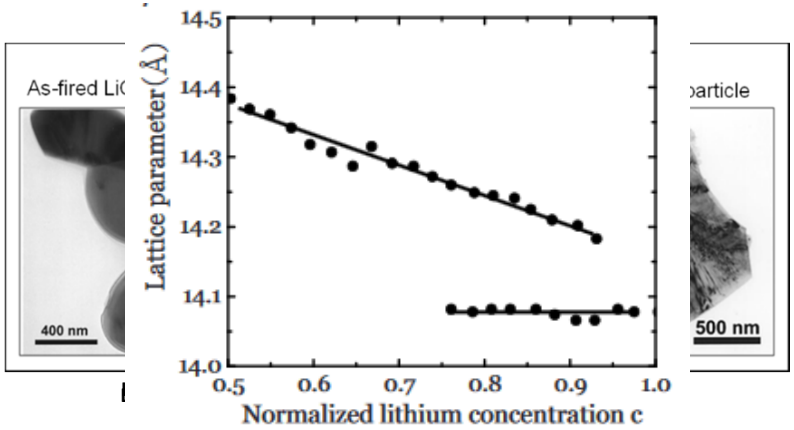

K. Zhao et al *J. Appl. Phys.* 108 (2010) 073517-1 - 073517-6
J. Reimers and J. Dahn *J. Electrochem. Soc.* 139 (1992) 2091 - 2097

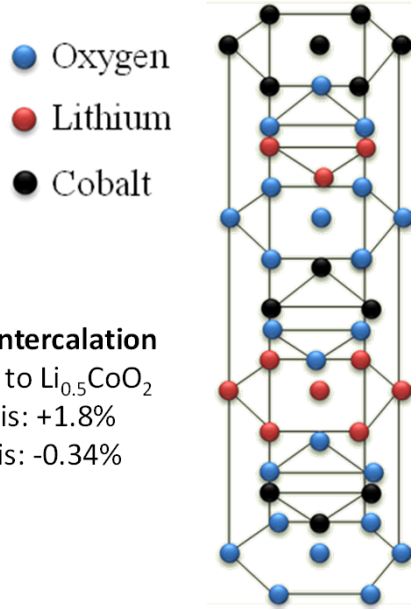

Li^+ de-intercalation
$LiCoO_2$ to $Li_{0.5}CoO_2$
c-axis: +1.8%
a-axis: -0.34%

Specific capacity: 137 mAh/g

$1\ Ah = 1\frac{C}{s}hr$= 3,600 C

$LiCoO_2$ = 97.87 g/mol

$Li \rightarrow Li^+ + e^-$

K. Mizushima et al. *J. Mater. Res. Bull.* 15 (1980) 783-789.

Degradation

CHEMICAL

Loss of Li^+ inventory

- SEI
- Side reactions of electrolyte

Impedance Rise

PHYSICAL

Loss of Active Material

- Particle isolation

Reduction of Electrode Utilization

- Anisotropic expansion/contraction
- Internal strains and dislocation defects
- Fracture of particles

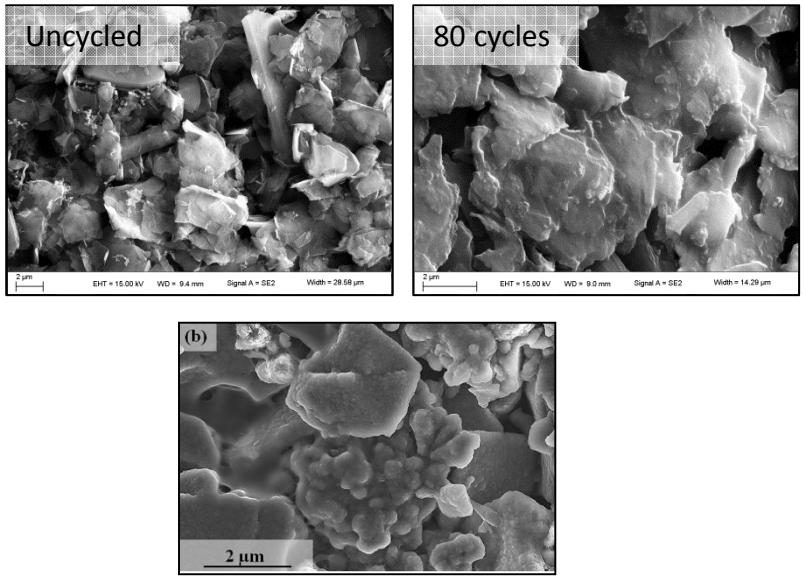

J. Lee et al. *Carbon* 52 (2013) 388-397

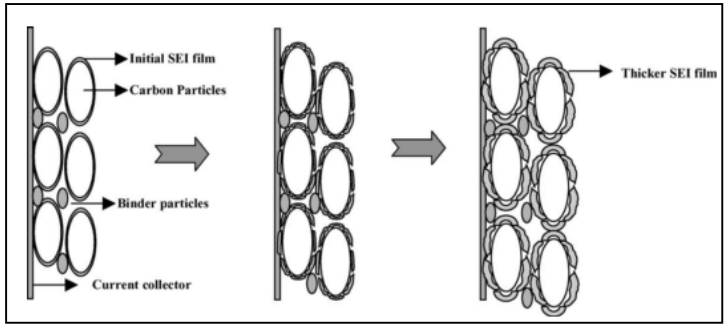

G. Ning et al. *J. Power Sources* 117 (2003) 160-169

Degradation

CHEMICAL

Loss of Li^+ inventory

- SEI
- Side reactions of electrolyte

Impedance Rise

PHYSICAL

Loss of Active Material

- Particle isolation

Reduction of Electrode Utilization

- Anisotropic expansion/contraction
- Internal strains and dislocation defects
- Fracture of particles

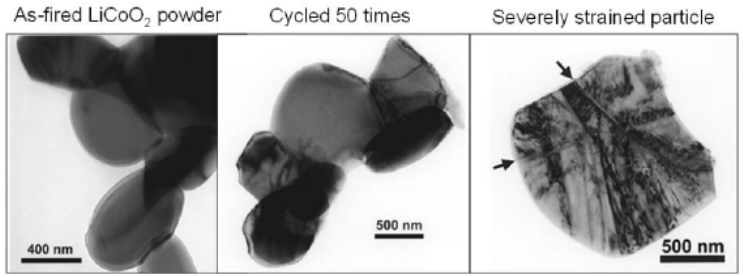

W. Haifeng et al. *J. Electrochem. Soc.* 146 (1999) 473-480

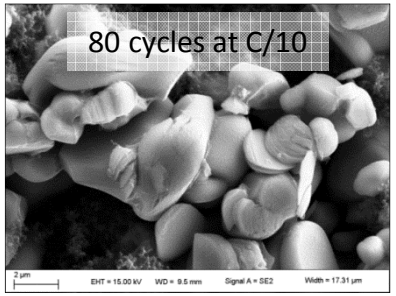

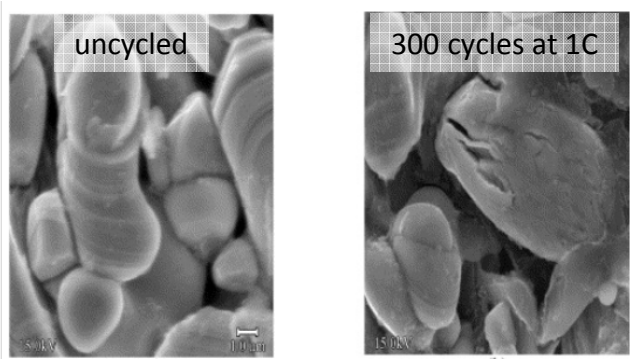

J. Li et al. *J. Power Sources* 102 (2001) 302-309

LIB TECHNOLOGY

DEGRADATION

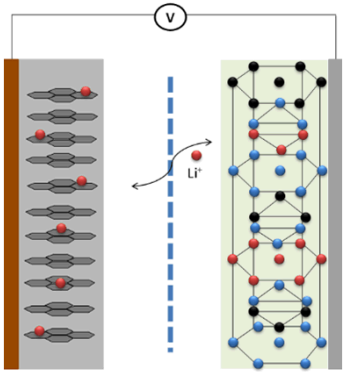

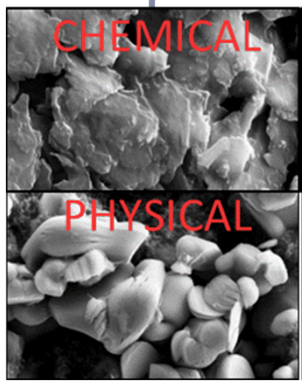

THESIS HYPOTHESIS

Project Approach

Hypothesis: Chemical mechanisms of degradation in a Li-ion battery dominate capacity loss at low c-rates, whereas mechanical-induced mechanisms dominate at high c-rates.

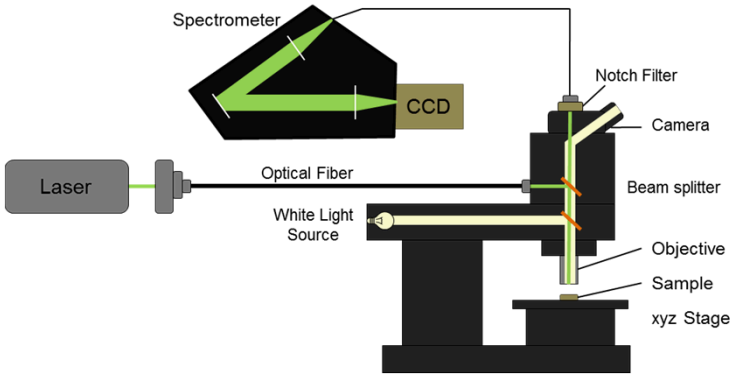

RAMAN SPECTROSCOPY

ELECTROCHEMICAL TESTING

MICROSCOPY

Coin Cells

Electrodes (Active:PVDF:CB)
Cathode: $LiCoO_2$ (94:3:3)
Anode: Graphite (92:6:2)

Electrolyte, 1.2 M $LiPF_6$ EC:EMC (3:7 by wt)

Separator, Celgard 2325

Potential Range, 3.0 V to 4.2 V

Constant Current (CC) or
Constant Current Constant Voltage (CCCV)

Temperature, 25°C

Cell Tester, Arbin BT2043

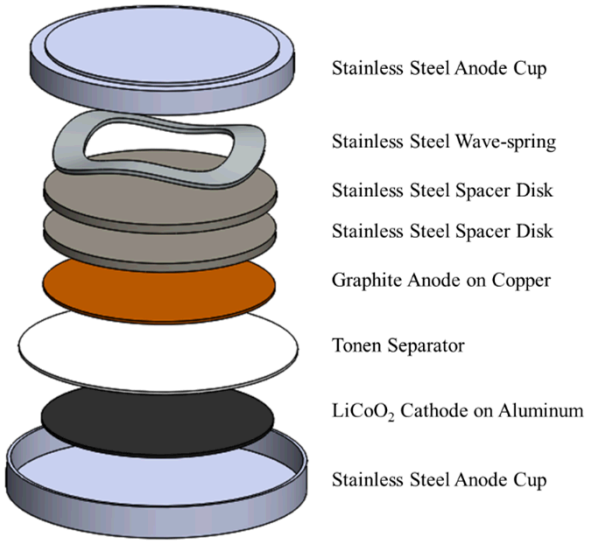

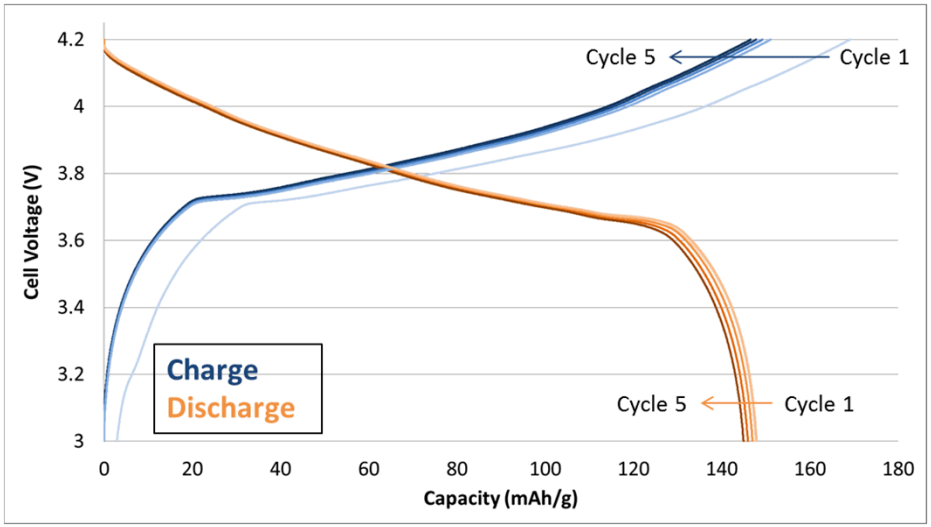

LIB TECHNOLOGY

DEGRADATION

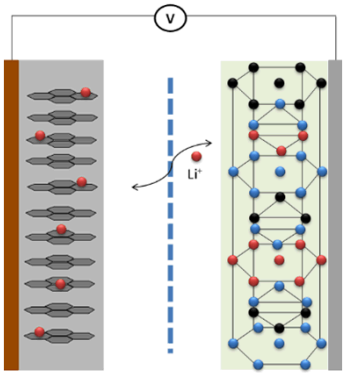

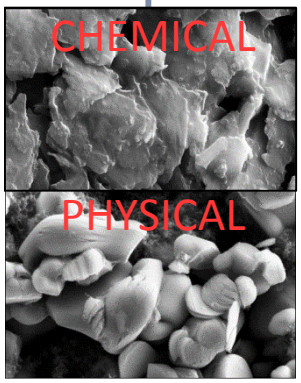

THESIS HYPOTHESIS

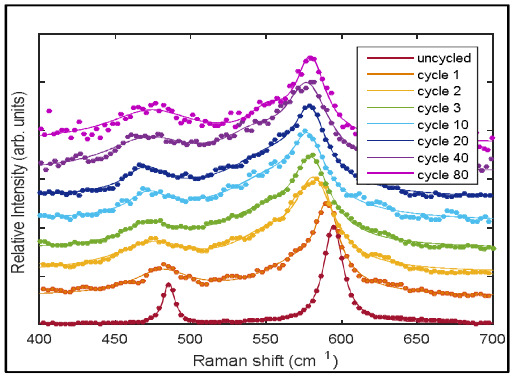

RAMAN SPECTROSCOPY

SEI Growth

- Hypothesis: At low c-rates chemical mechanisms dominate capacity fade
- SEI growth results in lithium inventory loss and impedance rise

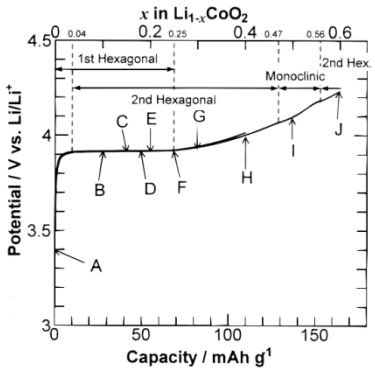

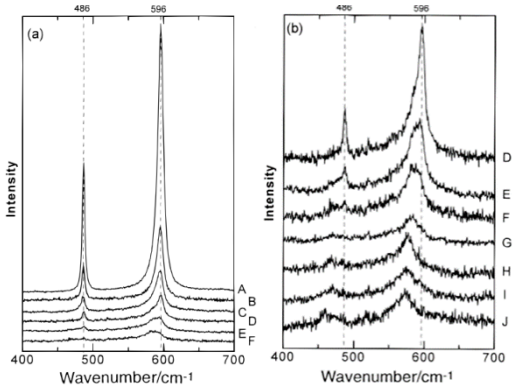

M. Inaba et al. *J. Raman Spectrosc.* 28 (1997) 613-617

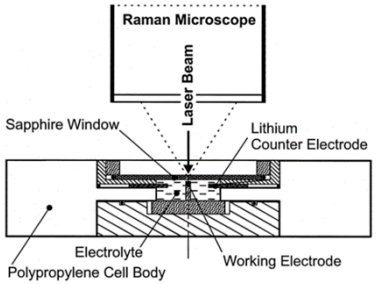

P. Novak et al. *J. Power Sources* 90 (2000) 52-58

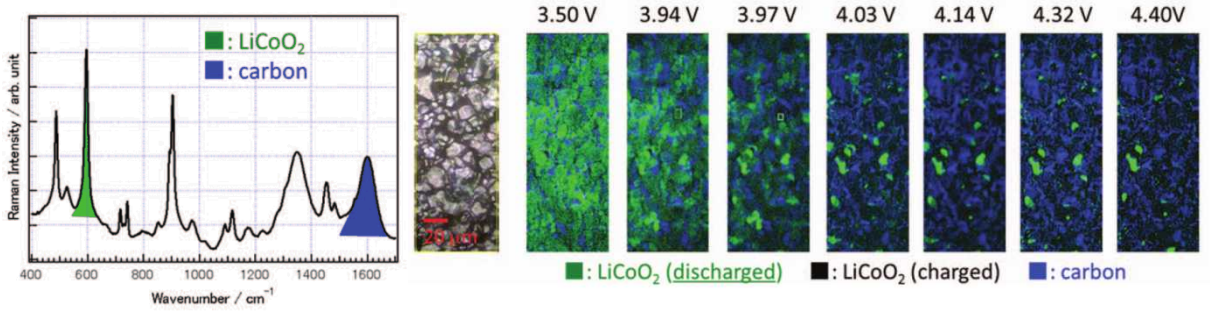

T. Nishi et al. *J. Electrochem. Soc.* 160 (2013) A1785-A1788

Experimental Setup

Develop Model:

1. Formation Cycle Test (Cycle 1 and 2)
2. State of Charge Test (Cycle 4)

Implement:

3. Long Term Cycle Test (Cycle 10, 20, 40, 80)

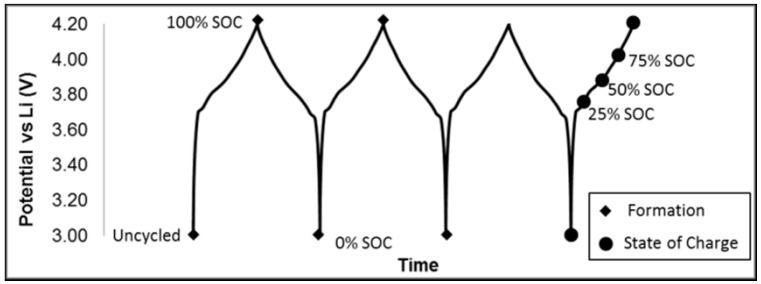

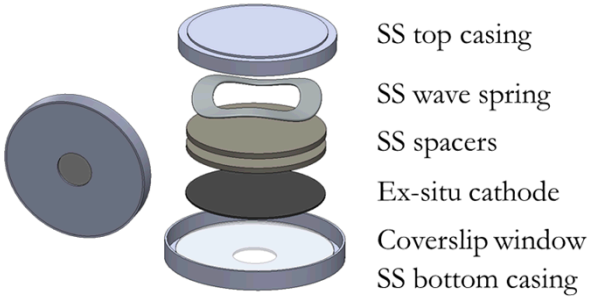

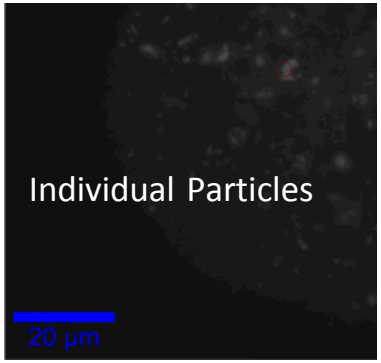

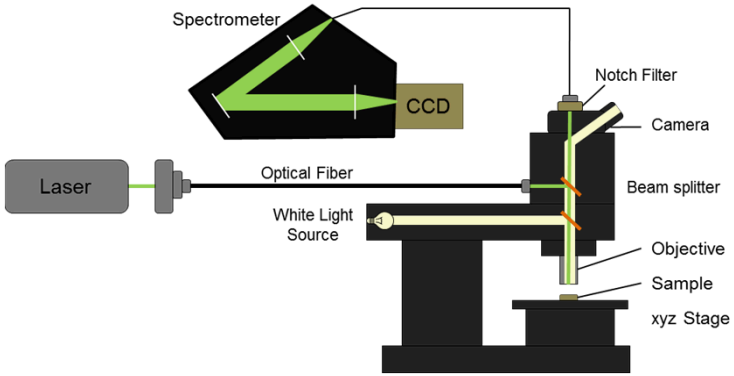

Cycle Information

C-rate : C/10

Raman Analysis Information

System: Witec Alpha 200R

Laser: Nd:YAG at 532 nm

Objective: 50 x , 0.55 NA (600 nm spot size)

Power : 250 µW

Integration time : 20 s integration, 15 accumulations

Snyder et al. *Journal of The Electrochemical Society* 163 (6) A1036-A1041 (2016)

Raman Analysis

SOC Study → Formation Study → Assign x in Li_xCoO_2 → Fit Particle Spectrum → Determine Average State → Validate Model → Compare to Capacity Loss Data

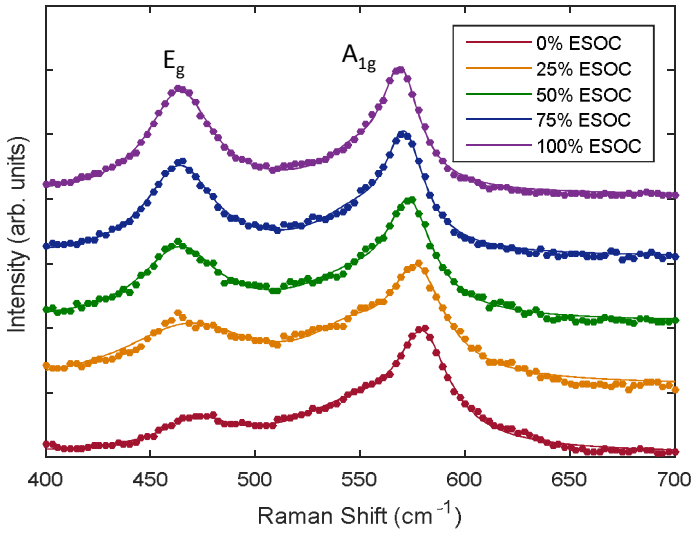

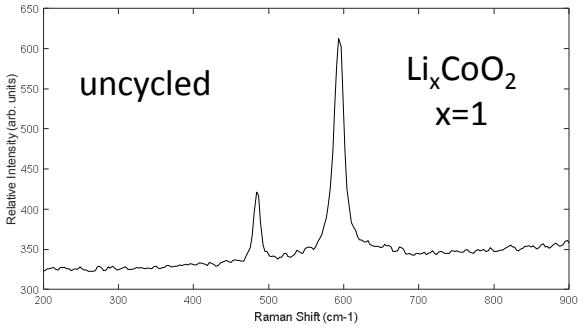

Lorentz Function

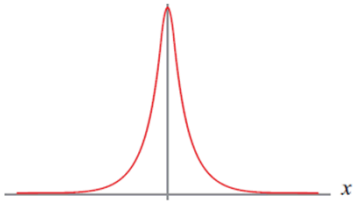

$$L(x) = A * \frac{1}{1 + \frac{(x-p)^2}{w^2}}$$

A ~ Amplitude
w ~ line width
p ~ peak position

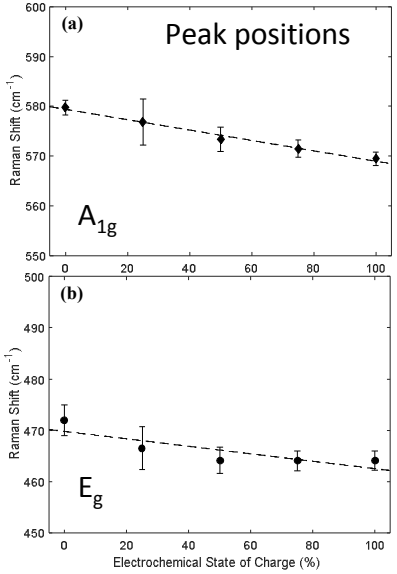

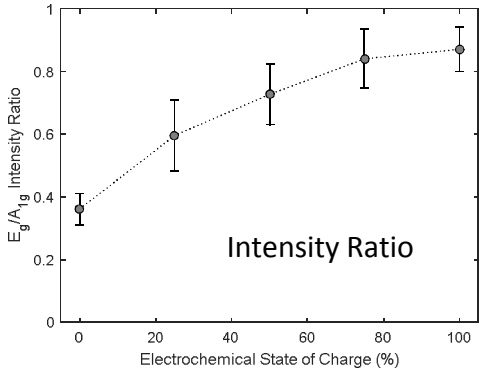

Snyder et al. *Journal of The Electrochemical Society* 163 (6) A1036-A1041 (2016)

Raman Analysis

SOC Study → **Formation Study** → Assign x in Li_xCoO_2 → Fit Particle Spectrum → Determine Average State → Validate Model → Compare to Capacity Loss Data

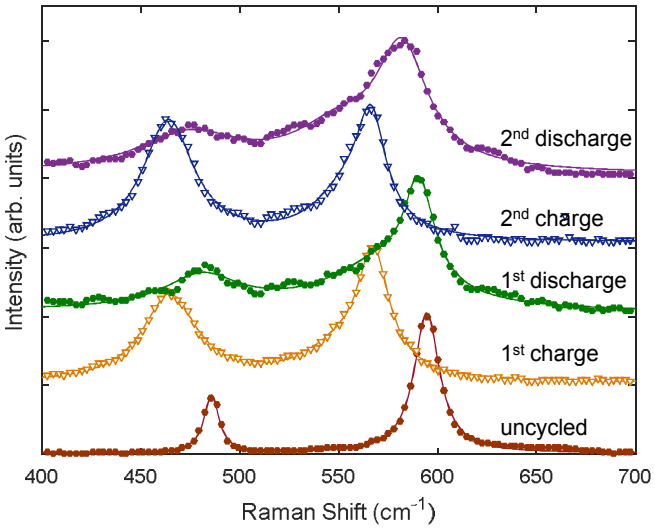

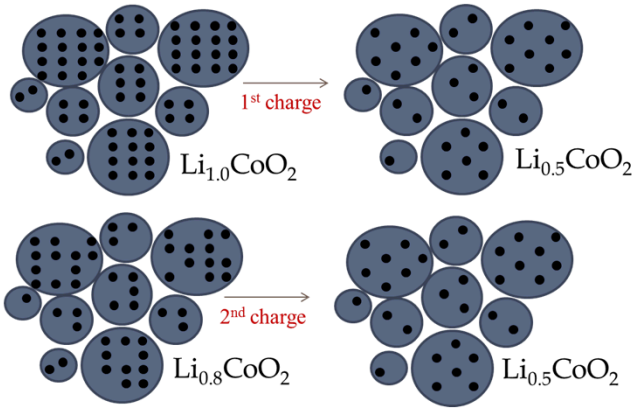

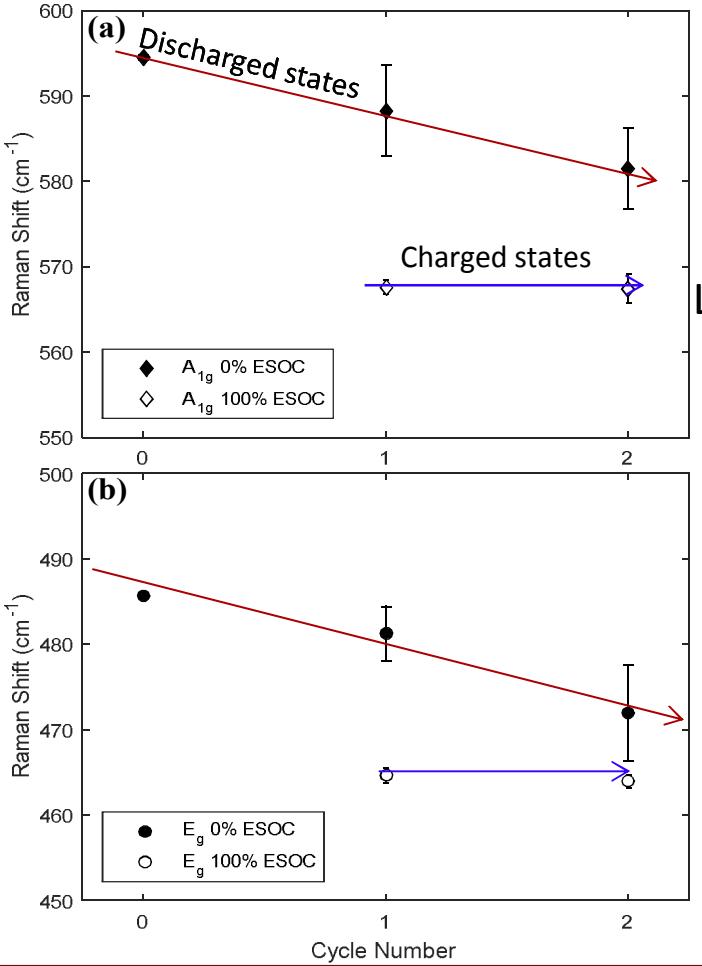

Li_xCoO_2

$Li_{0.5}CoO_2$

Raman Analysis

SOC Study → Formation Study → Assign x in Li_xCoO_2 → Fit Particle Spectrum → Determine Average State → Validate Model → Compare to Capacity Loss Data

Discharge Capacity Normalized to Theoretical Capacity

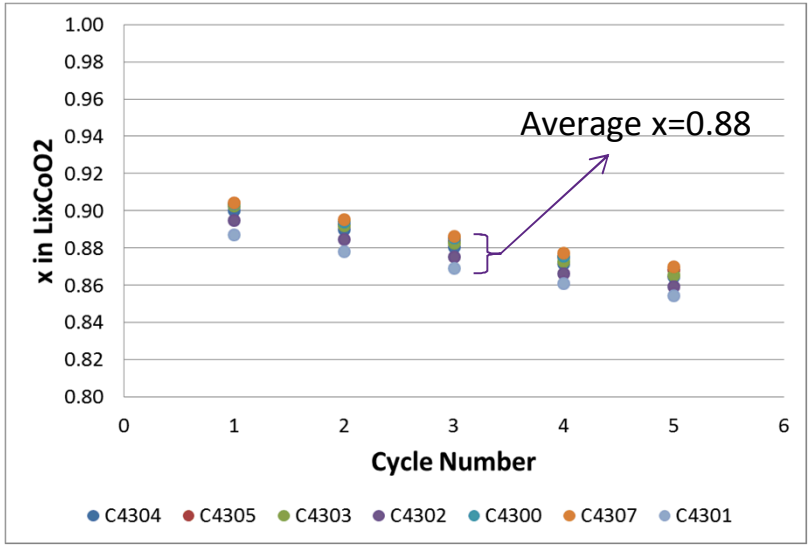

Assignment of lithiation state

ESOC (%)	x in Li_xCoO_2	PSOC (%)
0	0.88	24
25	0.785	43
50	0.69	62
75	0.595	81
100	0.5	100

Raman Analysis

SOC Study → Formation Study → Assign x in Li_xCoO_2 → **Fit Particle Spectrum** → Determine Average State → Validate Model → Compare to Capacity Loss Data

1. Preprocessing
   - Exclude data outside 400-700 cm^{-1}
   - Linear Background Removal
   - Cosmic Ray Removal
   - Normalize Intensity
2. Fit to Linear Combination of SOC spectra - use weights in peak regions to maximize fit
3. Compare Average Fit to Average Data – ensure fits represent the data well
4. Export coefficients and R^2 fit value

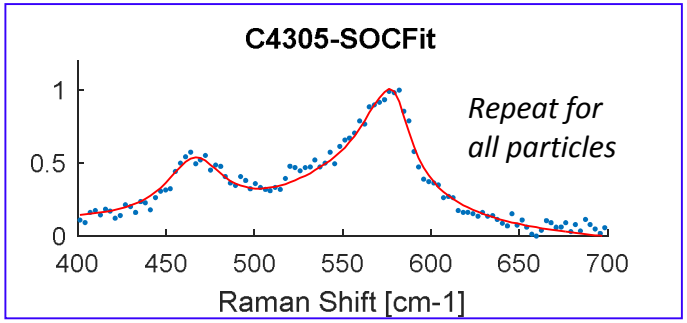

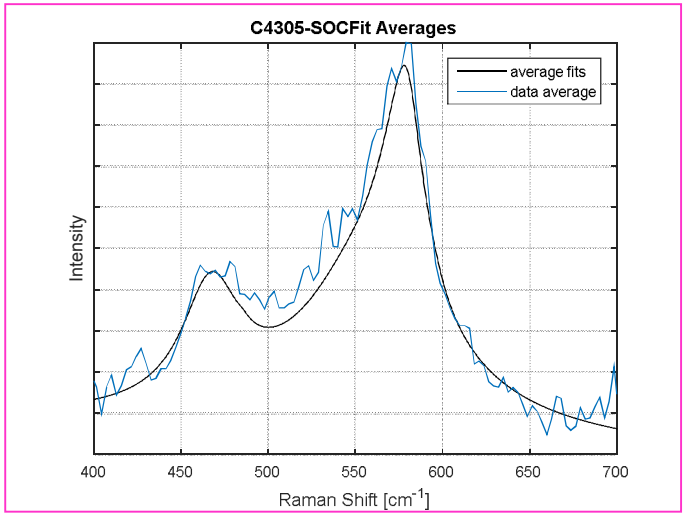

Raman Analysis

SOC Study → Formation Study → Assign x in Li_xCoO_2 → Fit Particle Spectrum → **Determine Average State** → Validate Model → Compare to Capacity Loss Data

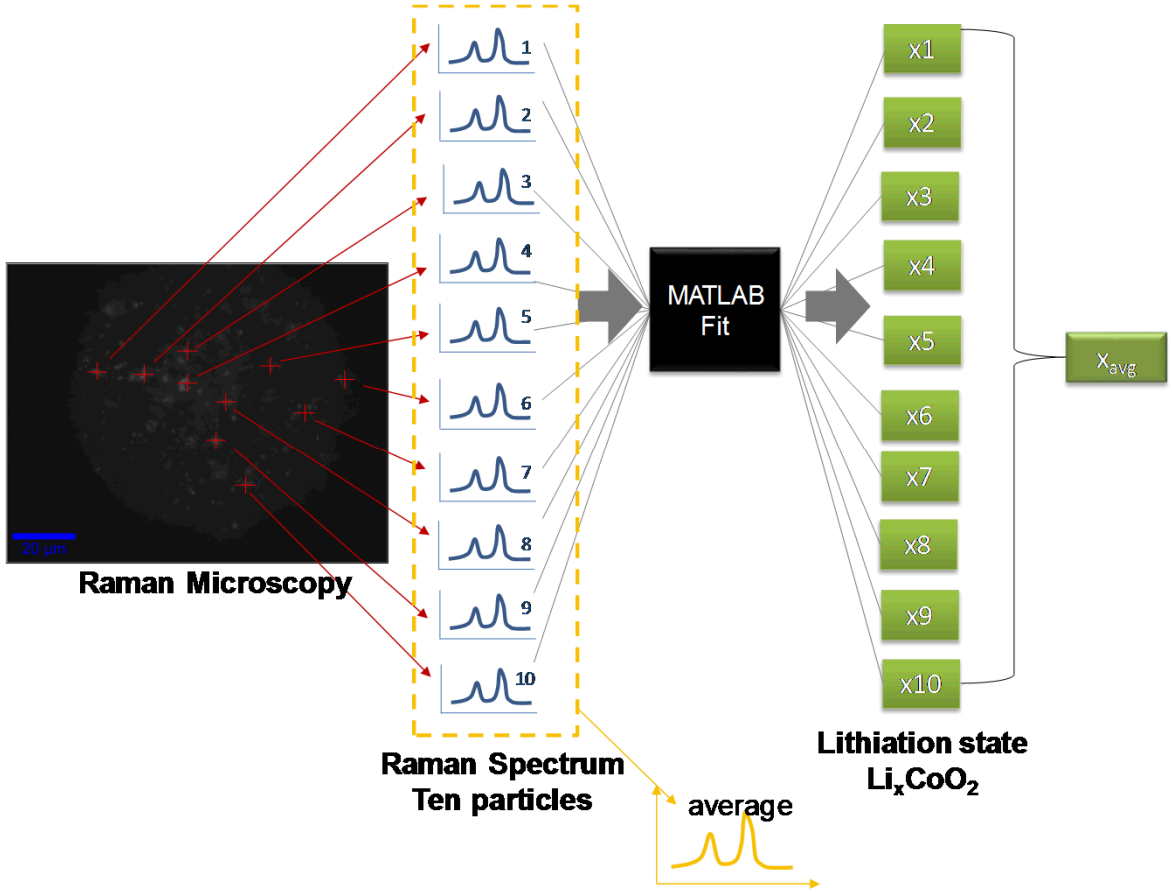

Raman Analysis

SOC Study → Formation Study → Assign x in Li_xCoO_2 → Fit Particle Spectrum → Determine Average State → **Validate Model** → Compare to Capacity Loss Data

Raman vs Electrochemical

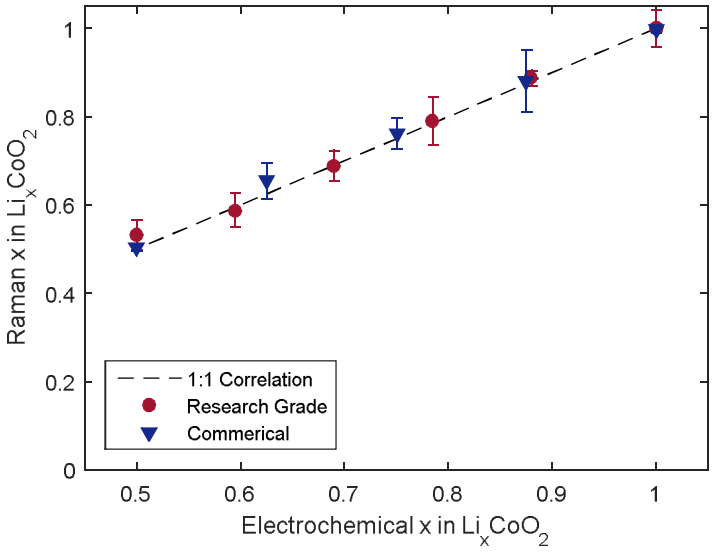

Research Grade

- SOC Samples

Commercial Electrodes

- Refreshed electrolyte (excess Li^+)

Snyder et al. *Journal of The Electrochemical Society* 163 (6) A1036-A1041 (2016)

Raman Analysis

SOC Study → Formation Study → Assign x in Li_xCoO_2 → Fit Particle Spectrum → Determine Average State → Validate Model → **Compare to Capacity Loss Data**

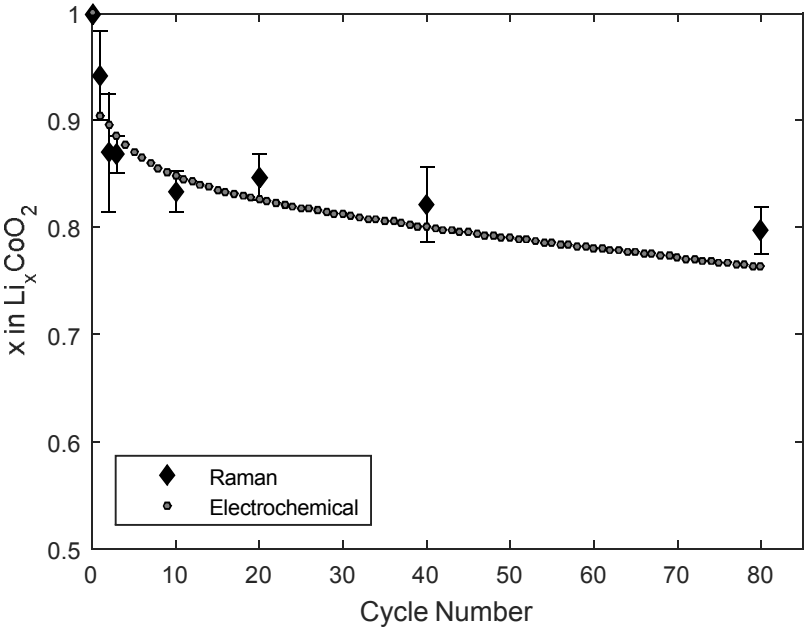

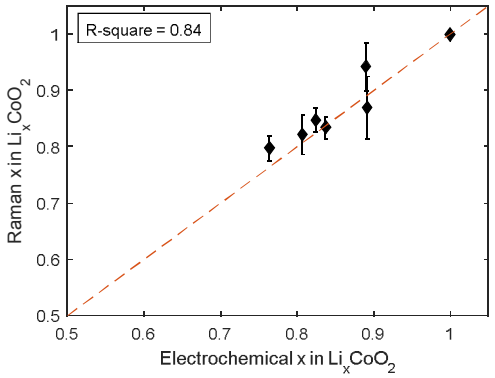

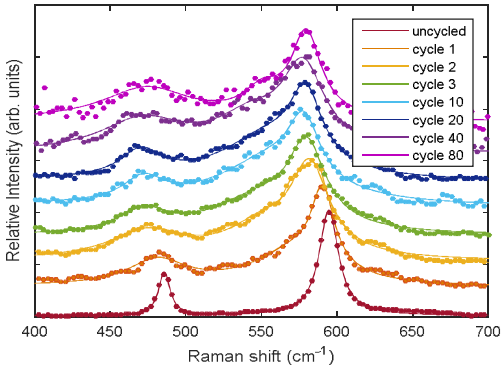

1. Raman microscopy is capable of estimating the lithiation state within individual $LiCoO_2$ particles
2. At these slow rates, capacity loss is exclusively caused by a loss of cycleable Li+
3. No "inactive" particles of LCO were found on the surface of the electrode
4. All particles were in a relatively homogenous state of lithiation at the slow rates (C/10)

Snyder et al. *Journal of The Electrochemical Society* 163 (6) A1036-A1041 (2016)

Raman Analysis

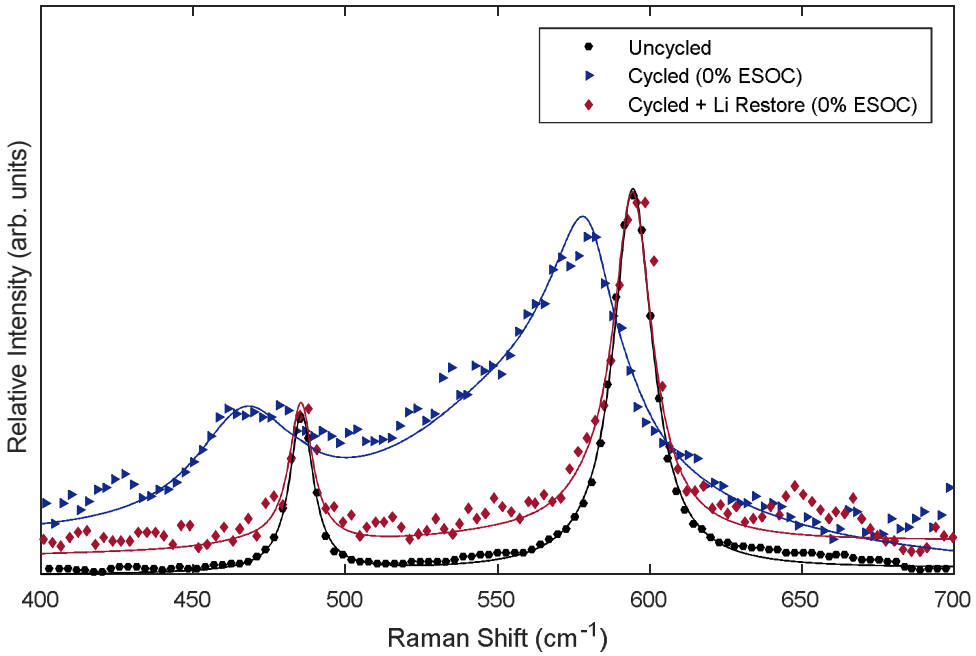

No measureable damage of $LiCoO_2$ structure that prohibits a fully lithiated state after cycling

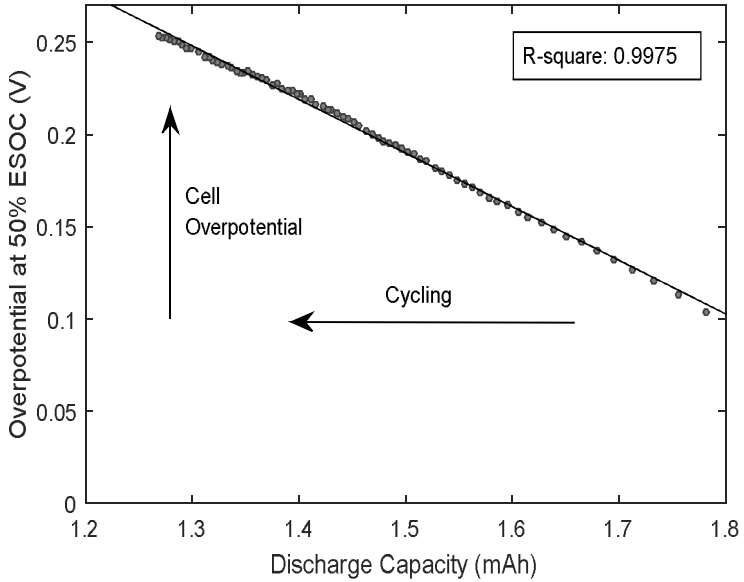

Overpotential rise is linked to continued SEI film formation/thickening which results in reduced Li^+ Inventory and thus capacity loss.

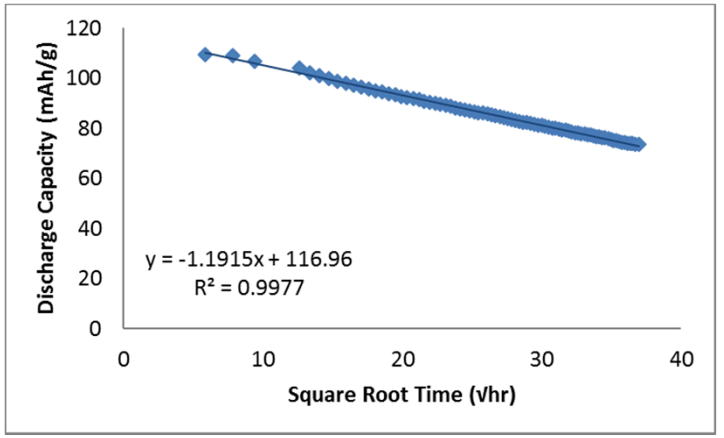

Snyder et al. *Journal of The Electrochemical Society* 163 (6) A1036-A1041 (2016)
Smith et al. *Journal of The Electrochemical Society* 158 (5) A447-A452 (2011)

LIB TECHNOLOGY

DEGRADATION

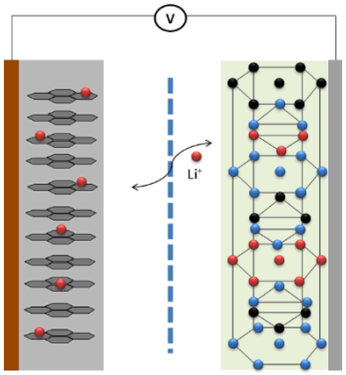

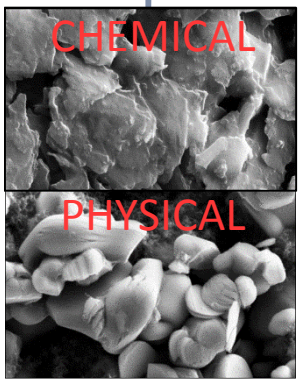

THESIS HYPOTHESIS

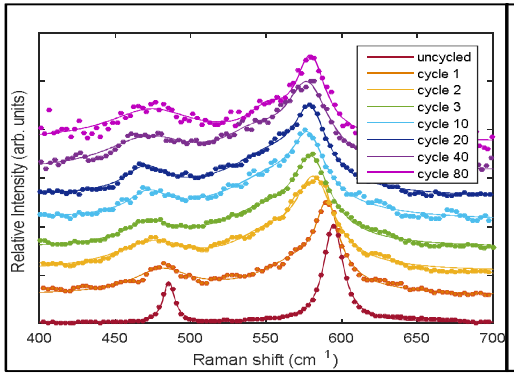

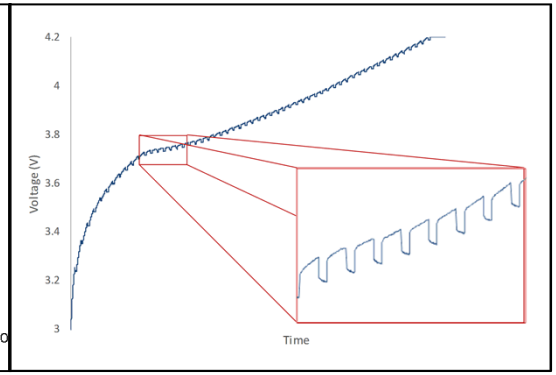

RAMAN SPECTROSCOPY

CURRENT INTERRUPT

Current Interrupt

Study Resistance Rise of Cells as function of c-rate : 1C, C/2, C/5, C/10

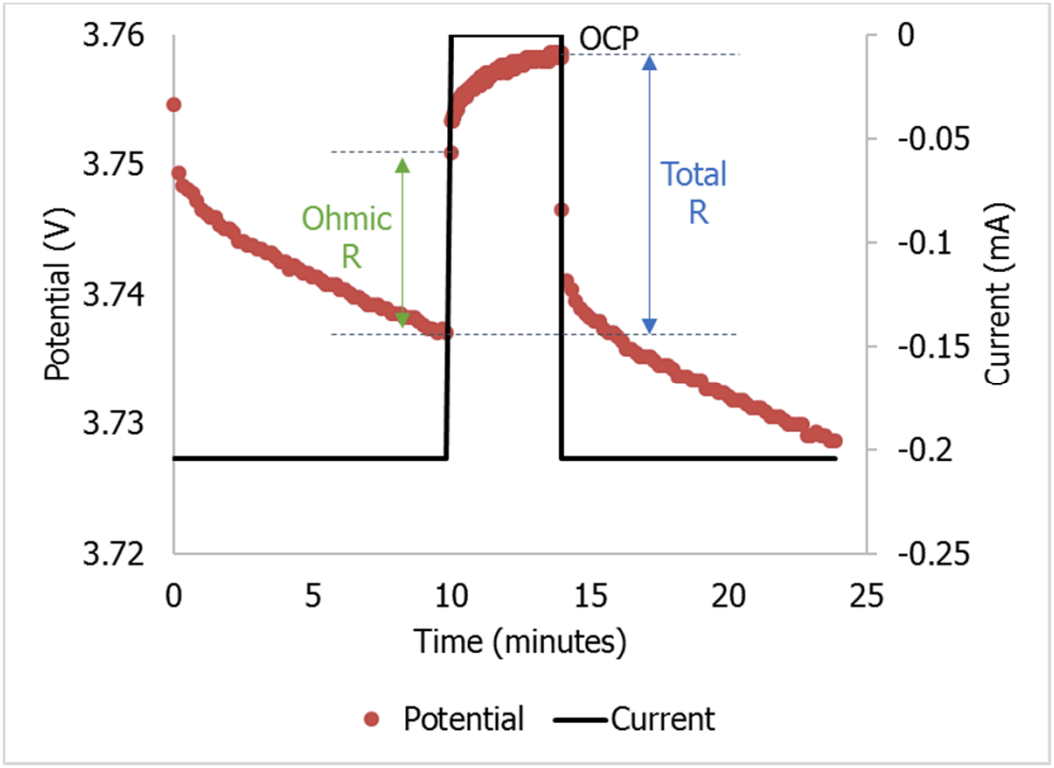

Total R

Ohmic (electronic)
Activation (Double layer)
Concentration (mass transport)

Test Setup

Rest Period: 4 min
CC Interval: Varies with c-rate

Resistance

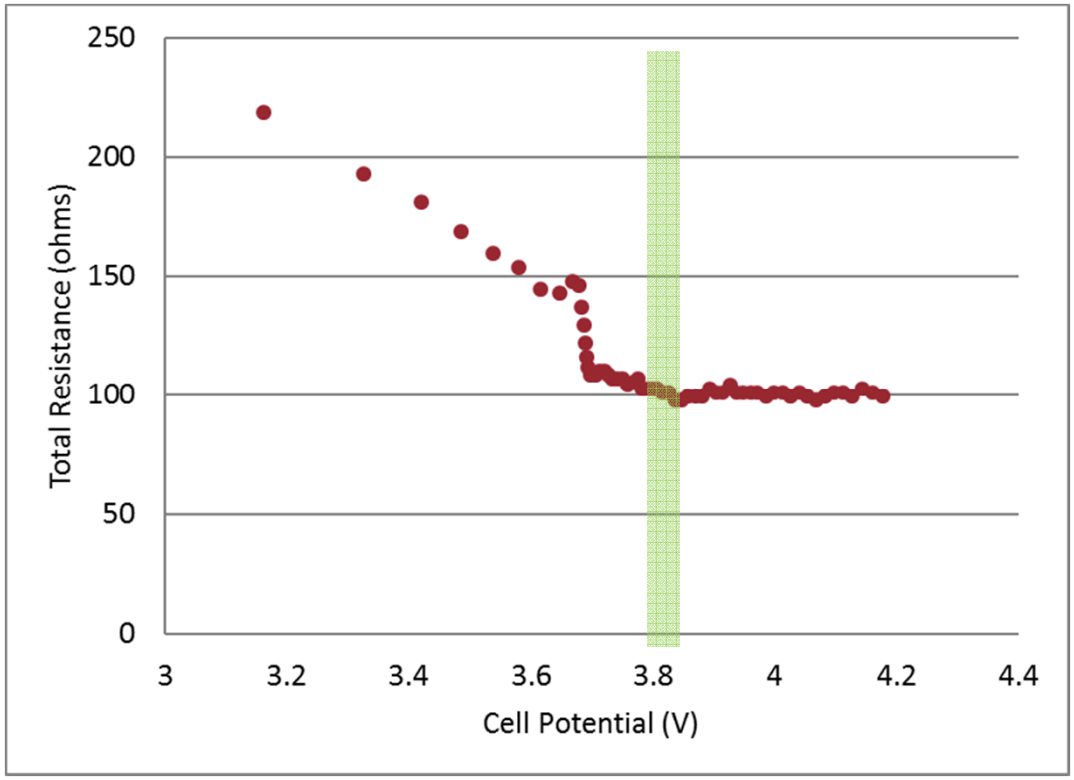

C/10 CCCV

$LiCoO_2$ /Li

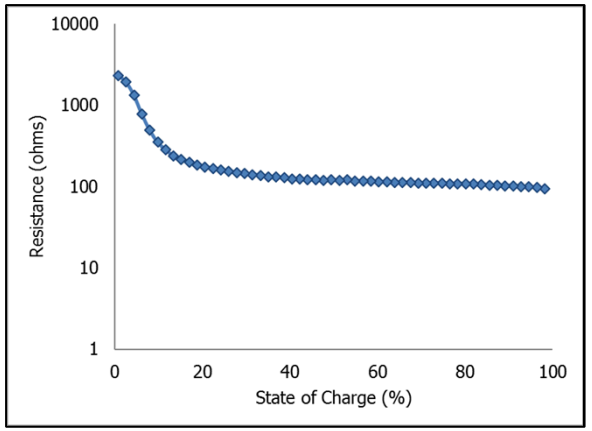

C/5 CCCV

Graphite /Li

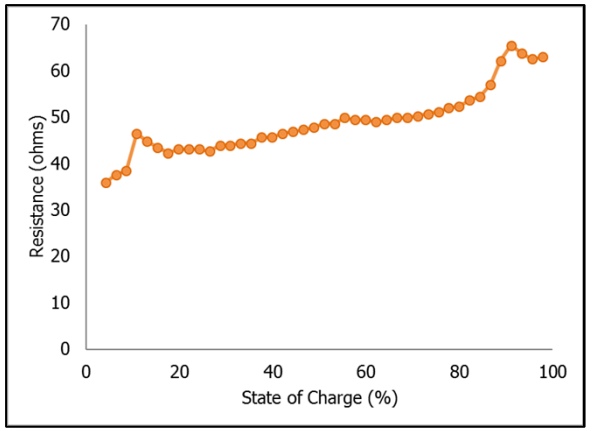

C/10 CCCV

Resistance Rise

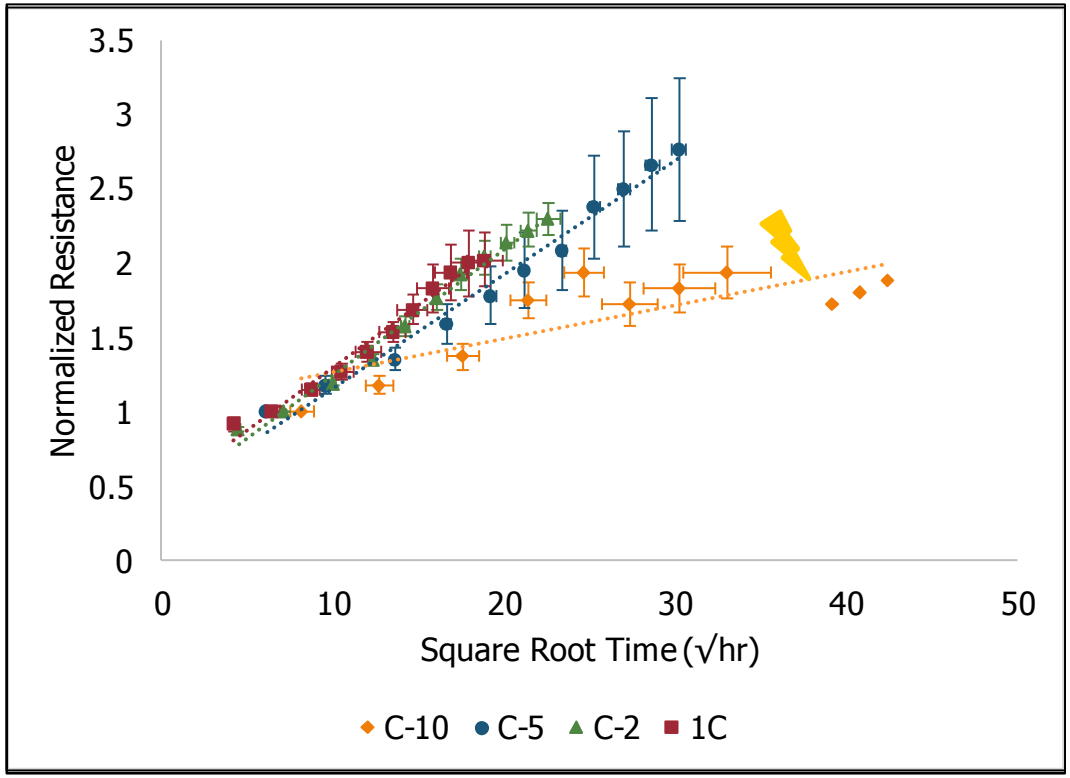

Cell Resistance Rise

- Electrolyte conductivity changes
- Film growth (√t)
- Binder conductivity changes

- Resistance rise is most impacted by chemical mechanisms as the rise correlates with √t and is relatively independent of c-rate

Capacity Loss

Capacity loss is c-rate sensitive and higher c-rates lead to faster capacity loss on a per cycle and time basis.

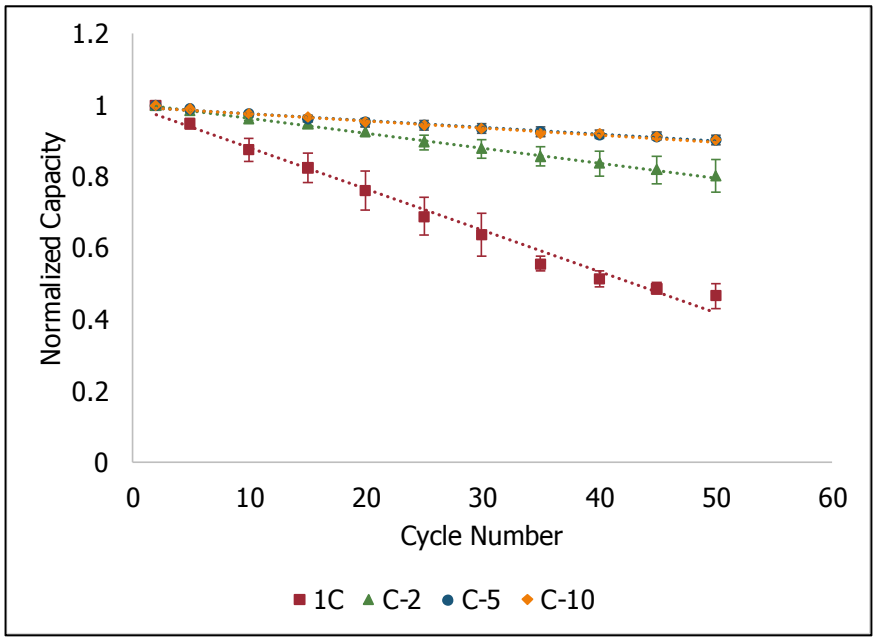

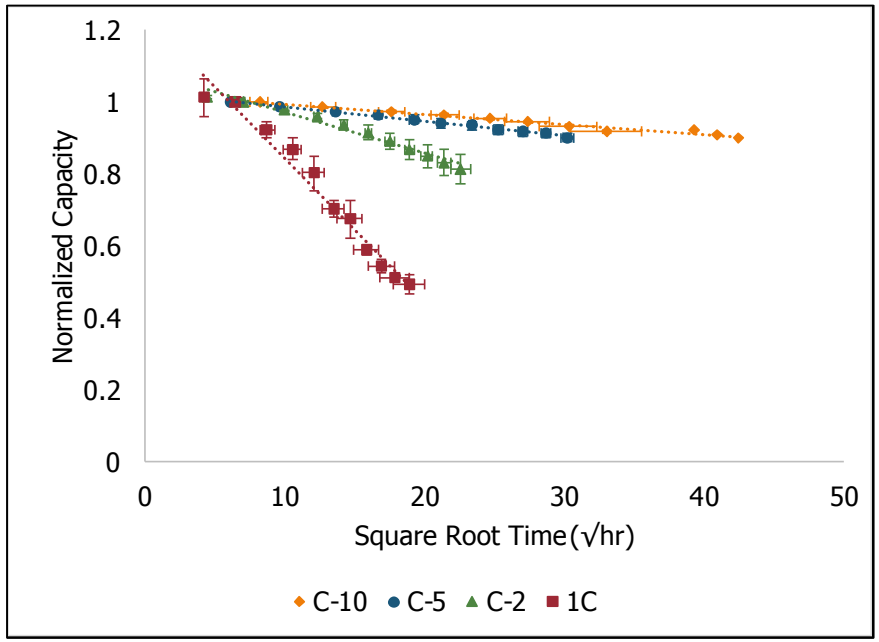

Cell Capacity loss

- Particle isolation
- Film growth (√t)
- Mechanical damage

Current Interrupt

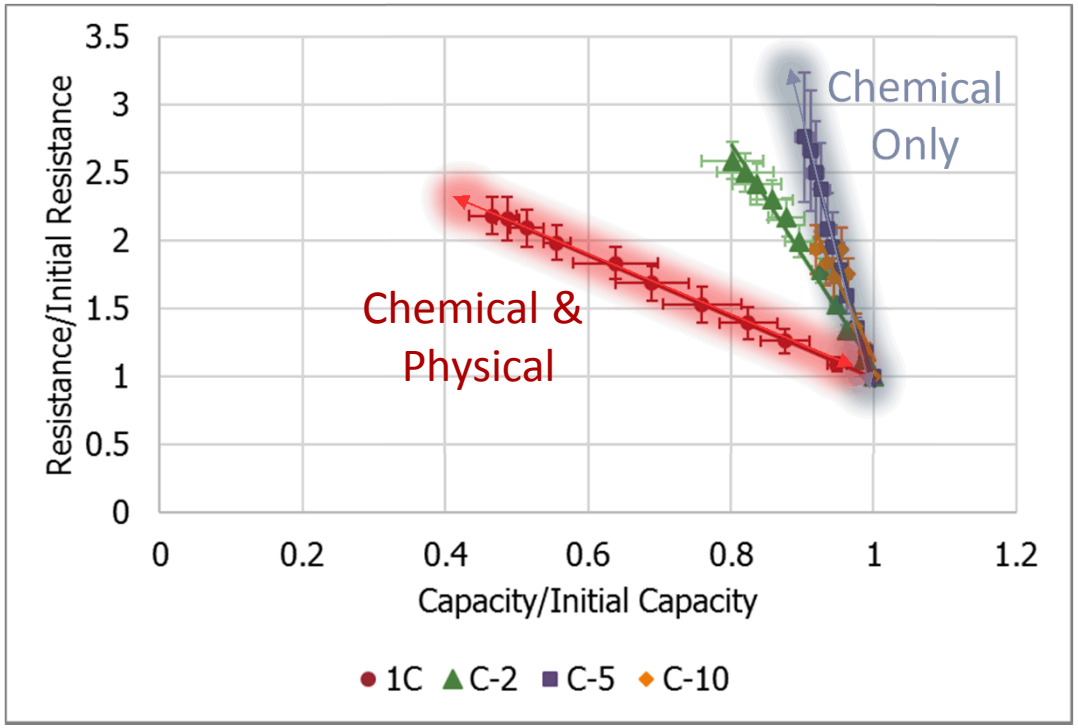

- Resistance measures chemical degradation
- Capacity loss stems from chemical and physical degradation
- As c-rate is increased, the contribution from physical degradation also increases

Particle Fracture

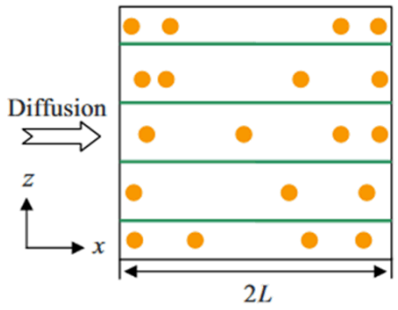

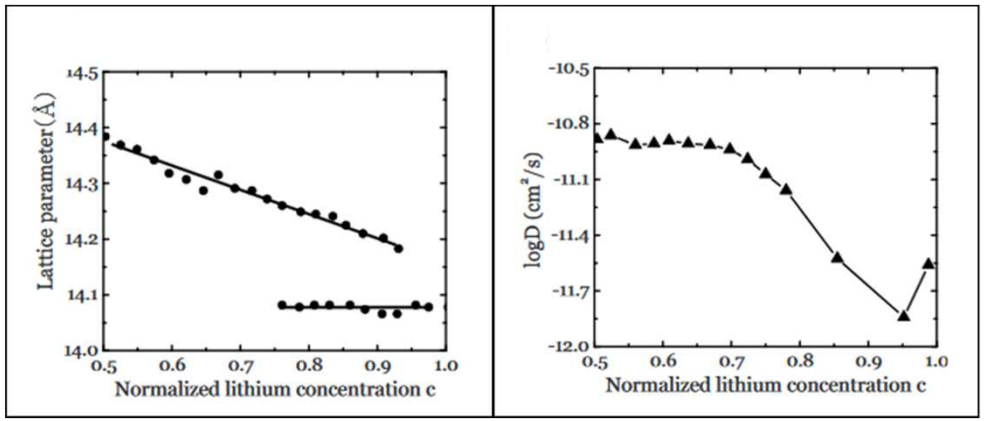

$$D = \frac{L^2}{t}$$ Concentration Gradients $$\varepsilon = \frac{l(c) - l_o}{l_o}$$

Crack Propagation

$$G = ZE\varepsilon^2 L$$

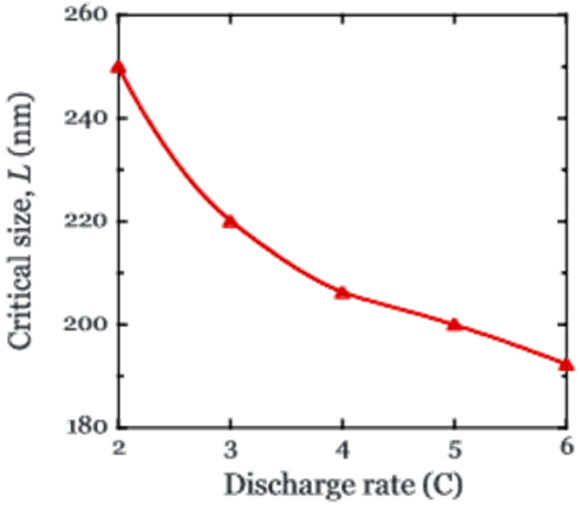

$$L_c = \frac{\Gamma}{Z_{max} E \varepsilon_m{}^2}$$

L_c: critical particle size
Γ: fracture energy of $LiCoO_2$
Z_{max}: maximum energy release
E: elastic modulus of $LiCoO_2$
ε_m: mismatch strain

Fracture Model: Zhao et al. J. Appl. Phys. 108 (2010) 073517-1
Diffusion Measurements: Xie et al. Solid State Ionics 179 (2008) 362
Lattice Constant Measurements: Reimers and Dahn J. Electrochem. Soc. 139 (1992) 2091

Particle Fracture

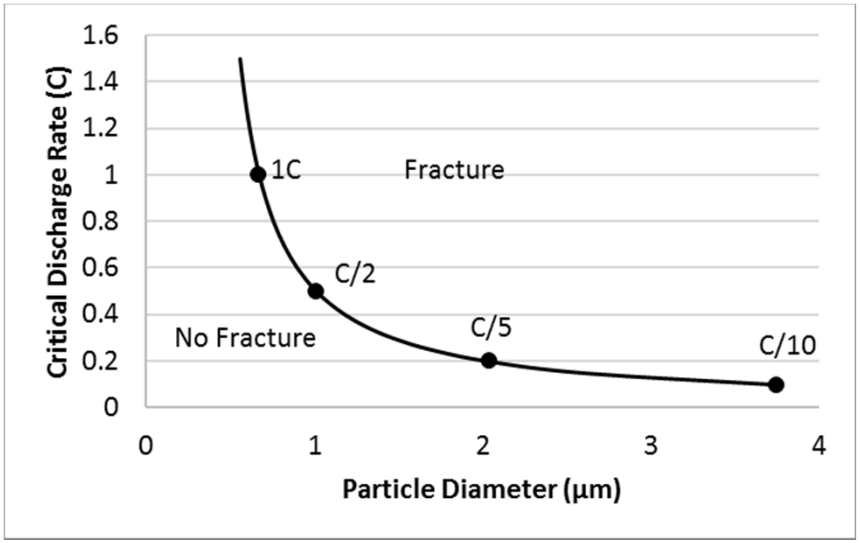

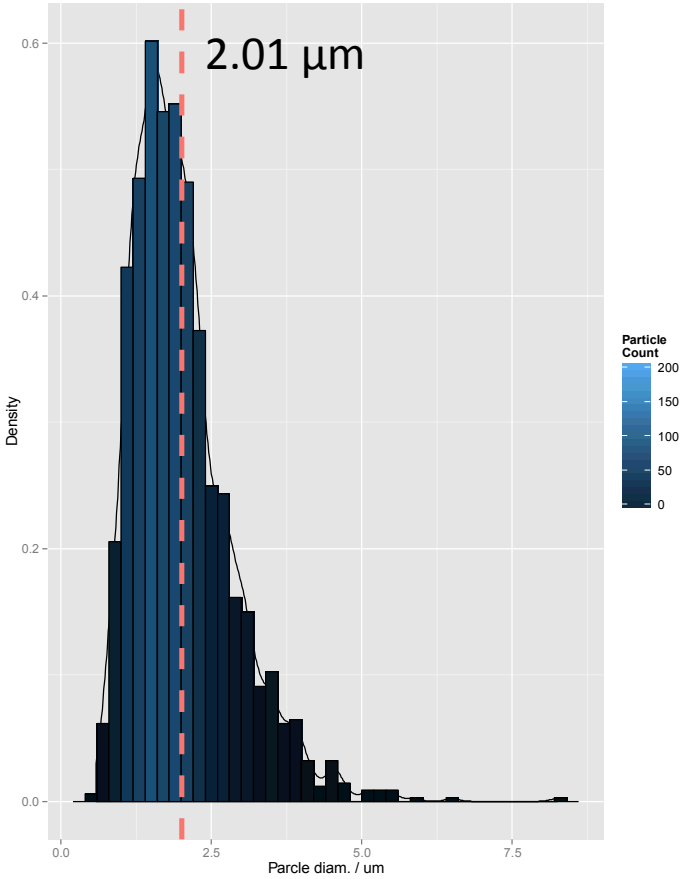

Courtesy of Dr. Farid El Gabaly (Sandia – CA)

Simulations support the increased likelihood of particle fracture with increased c-rate

K. Zhao et al *J. Appl. Phys.* 108 (2010) 073517-1 - 073517-6

LIB TECHNOLOGY

DEGRADATION

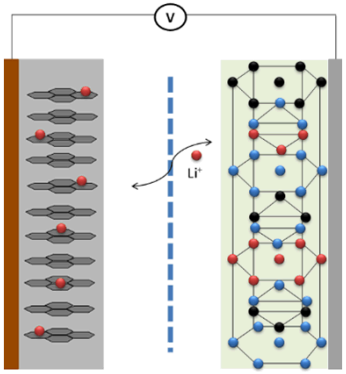

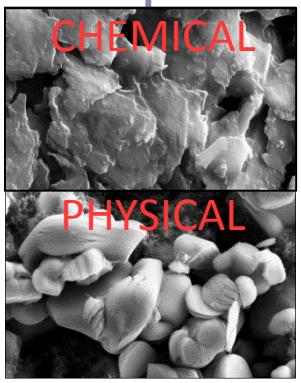

THESIS HYPOTHESIS

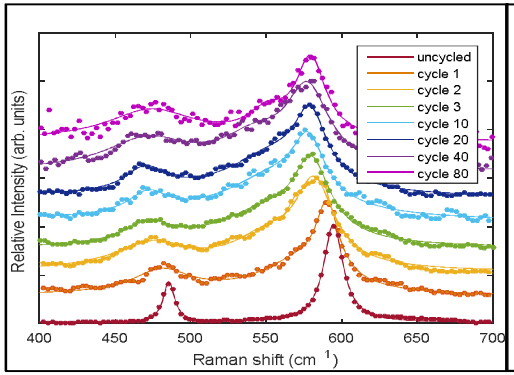

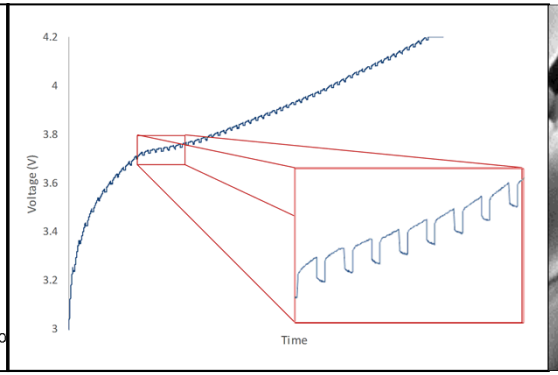

RAMAN SPECTROSCOPY

CURRENT INTERRUPT

MICROSCOPY

Microscopy analysis

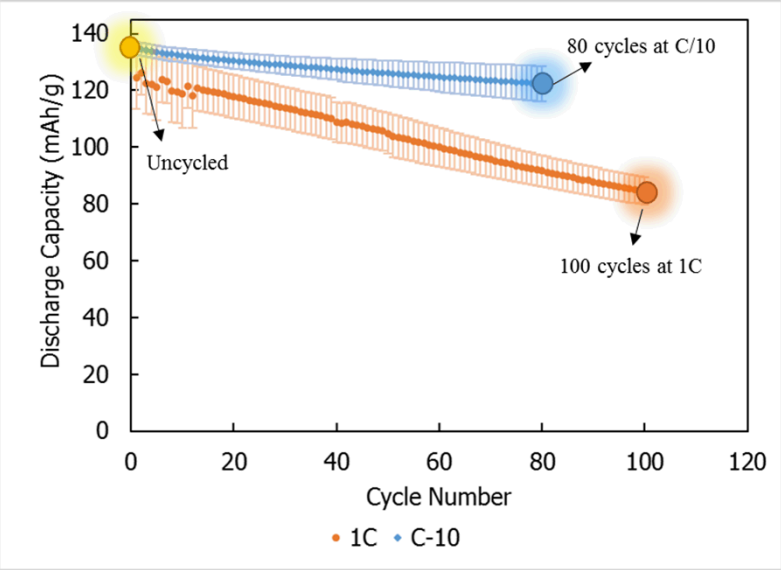

SEM
15 kV

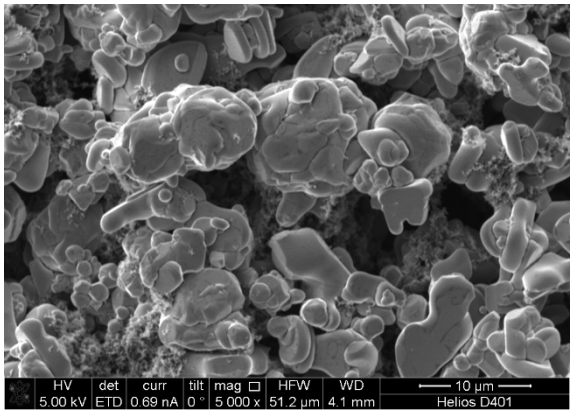

FIB Removal

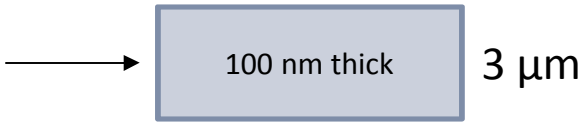

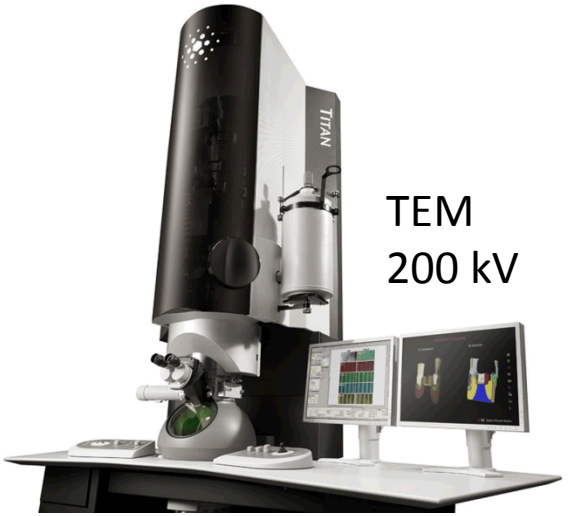

TEM
200 kV

Uncycled

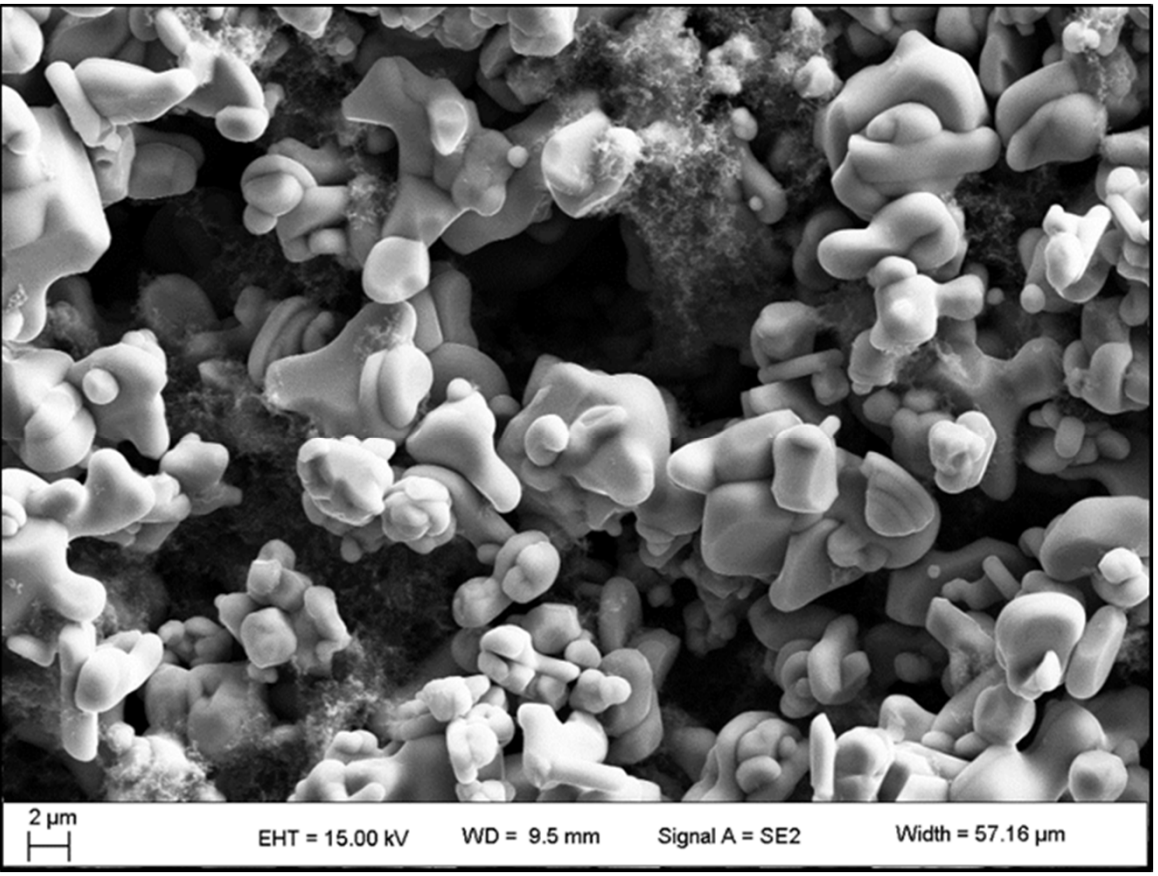
2 µm
EHT = 15.00 kV
WD = 9.5 mm
Signal A = SE2
Width = 57.16 µm

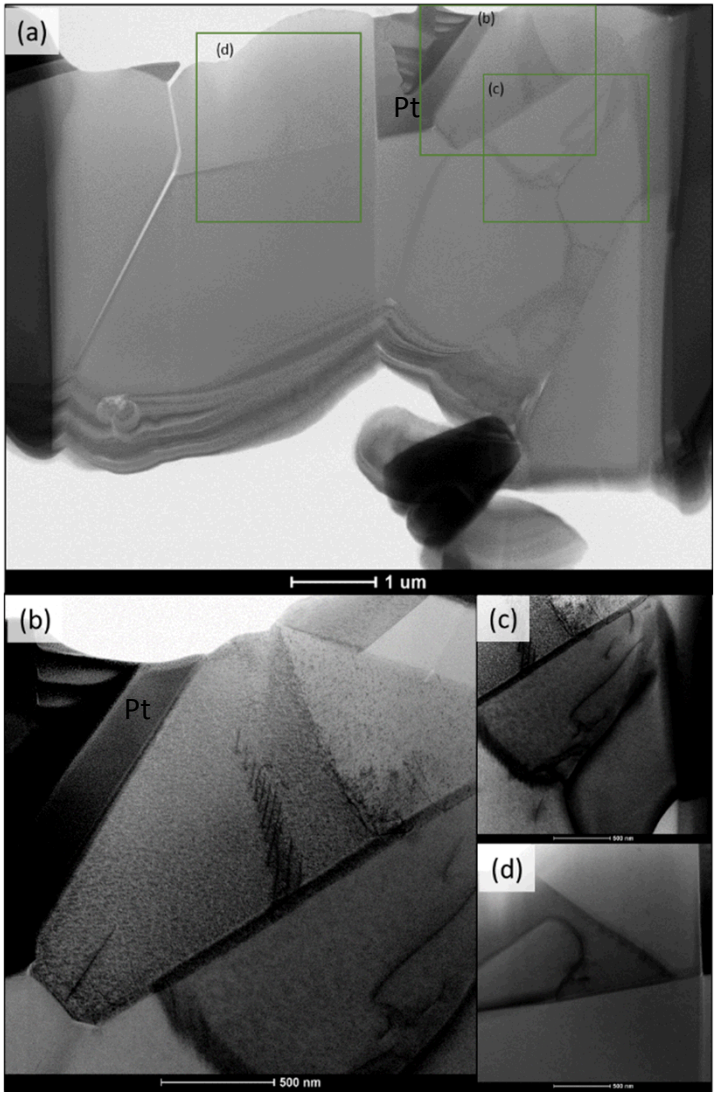
(a)
(b)
(c)
(d)
Pt
1 um
(b)
Pt
(c)
(d)
500 nm

80 cycles at C/10

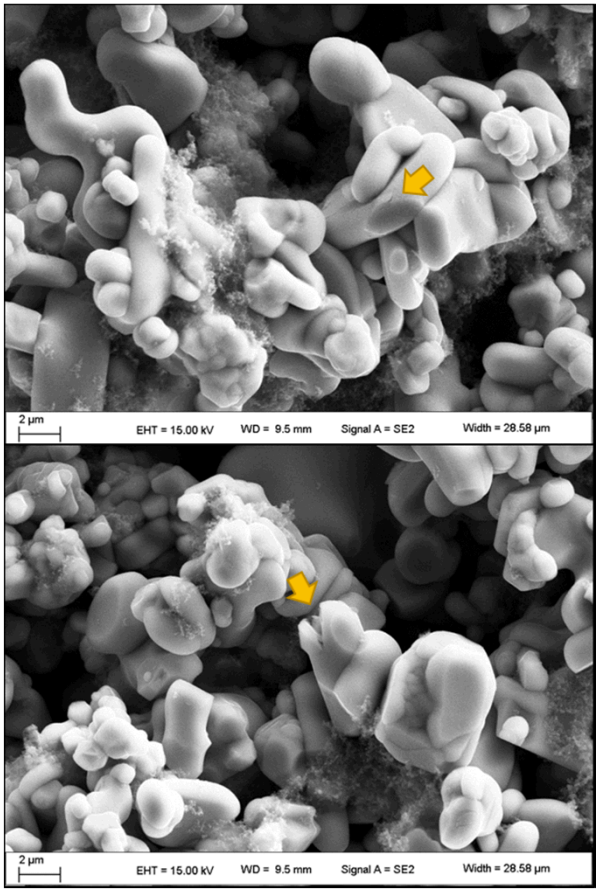

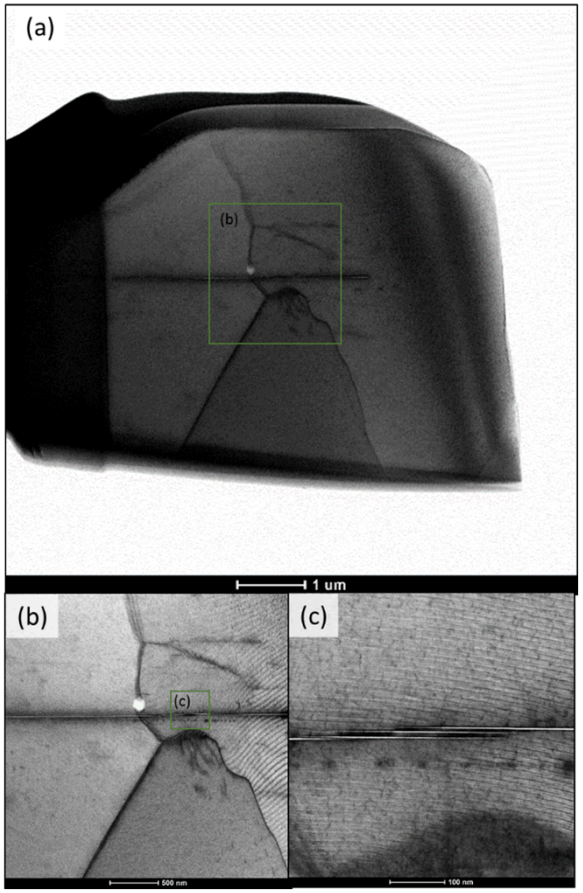

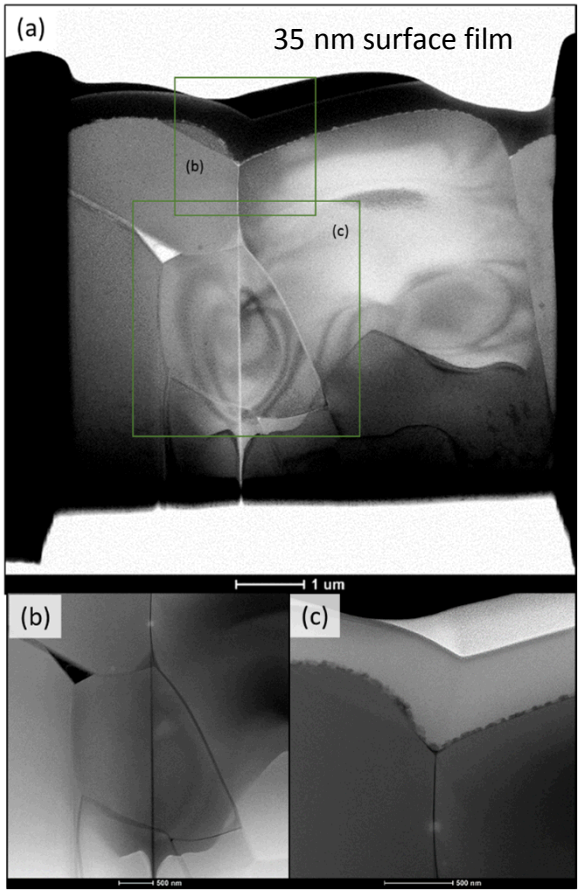

100 cycles at 1C

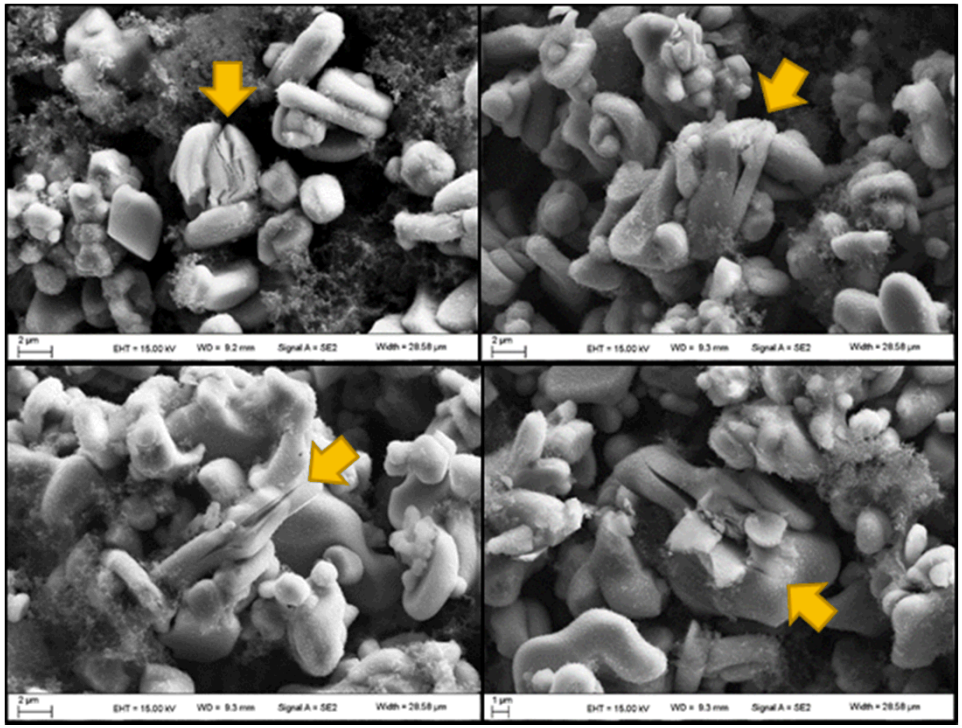

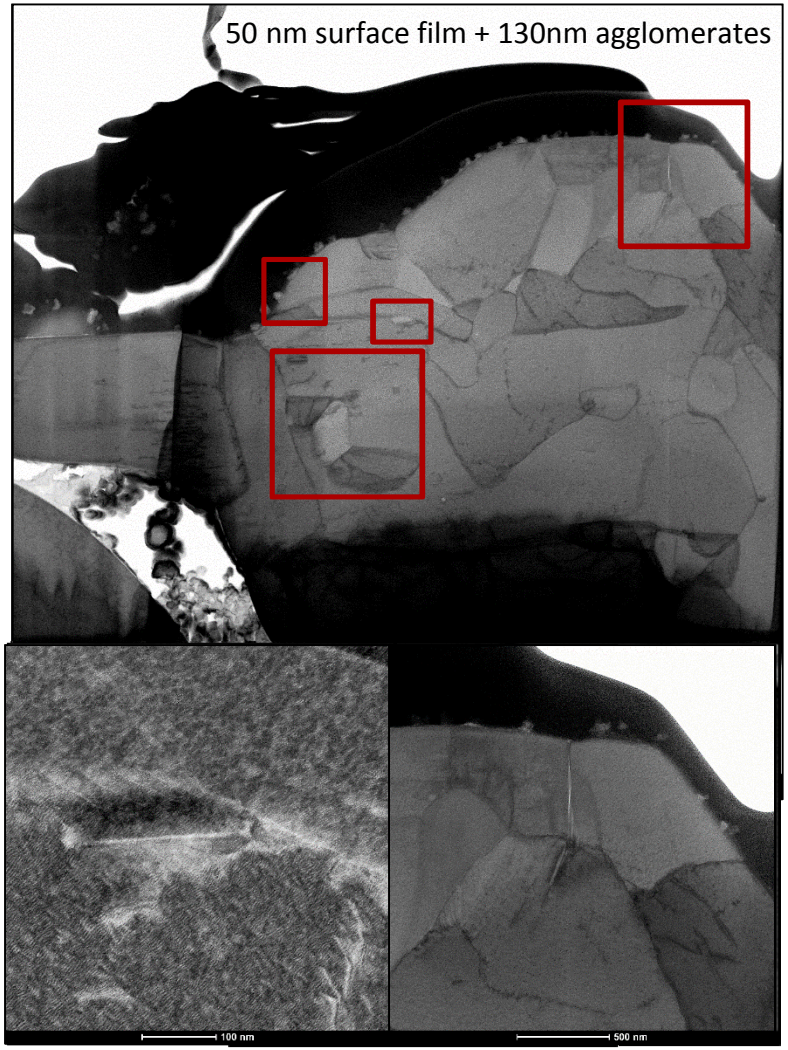

Damage is most extensive in high c-rate electrodes

Li ion transport changes

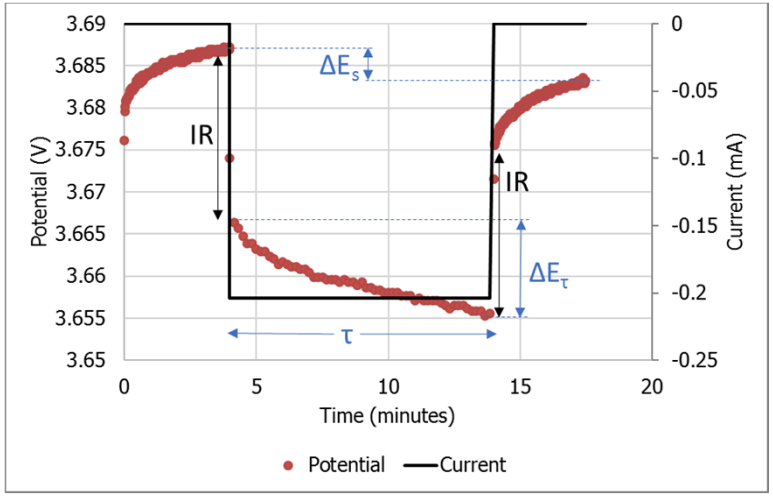

$$\widetilde{D}_{Li} = \frac{4}{\tau\pi}\left(\frac{m_B V_m}{M_B S}\right)^2\left(\frac{\Delta E_s}{\Delta E_\tau}\right)^2$$

m_B : mass of active material
V_m : molar volume
M_B : atomic weight
S : surface area

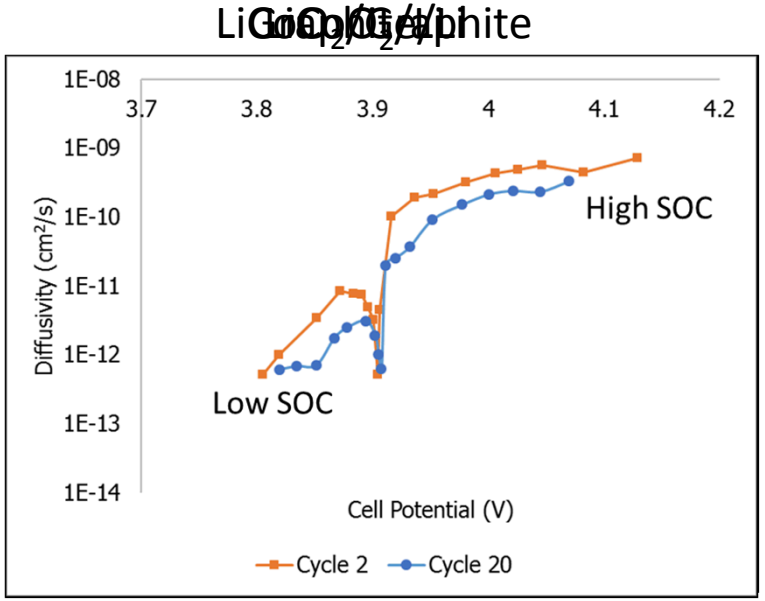

- Diffusivity degrades with cycling and is attributable to the $LiCoO_2$ electrode.
- Micro-cracks, high dislocation densities, and surface films are all expected to affect Li ion trapping and reduce Li ion transport

W. Weppner and R. Huggins *J. Electrochem. Soc.* (1977) 1569-1578.
A. Funabik et al. *J. Electrochem. Soc.* 145 (1998) 172-178.

LIB TECHNOLOGY

DEGRADATION

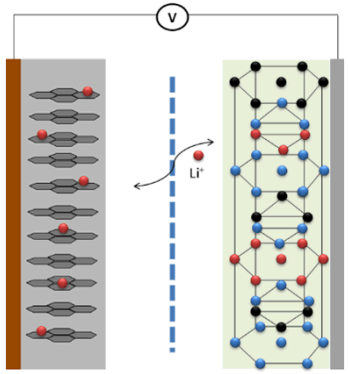

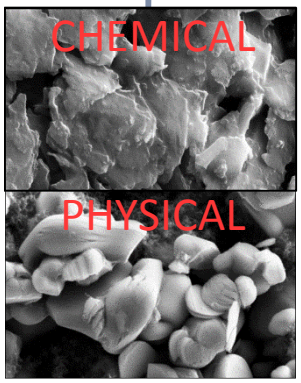

THESIS HYPOTHESIS

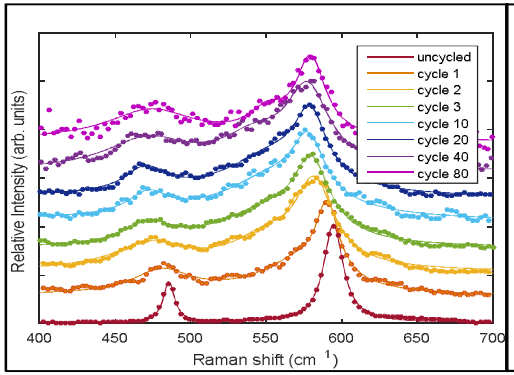

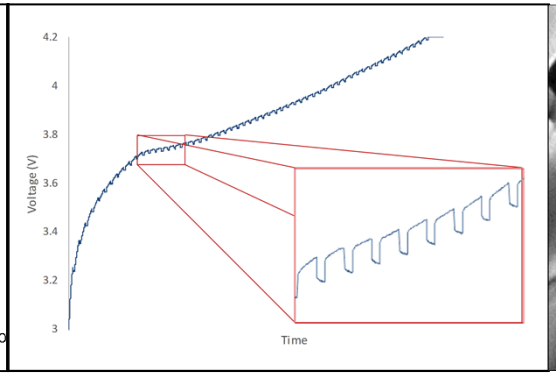

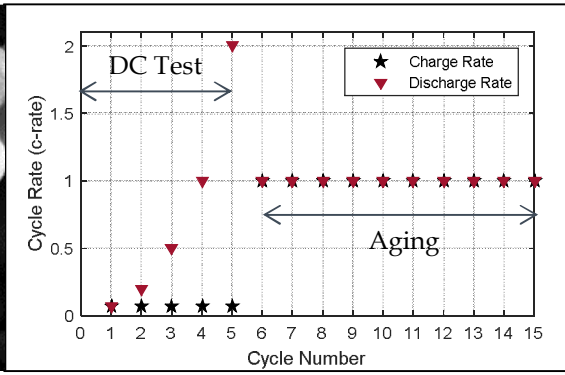

RAMAN SPECTROSCOPY

CURRENT INTERRUPT

MICROSCOPY

RATE CAPABILITY

Rate Capability Test Procedure

Tests electrode utilization at various rates and how it evolves throughout cycling

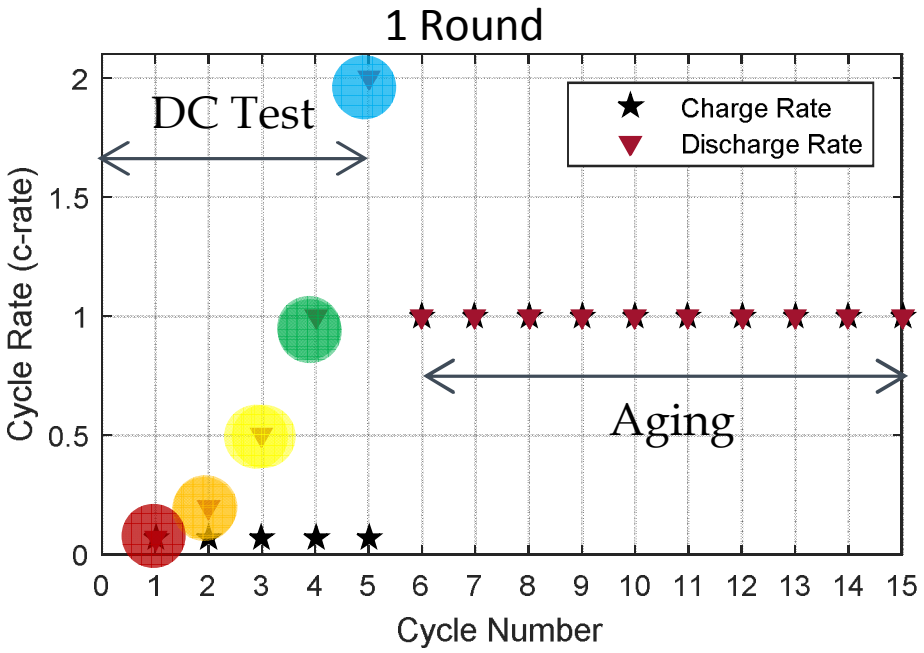

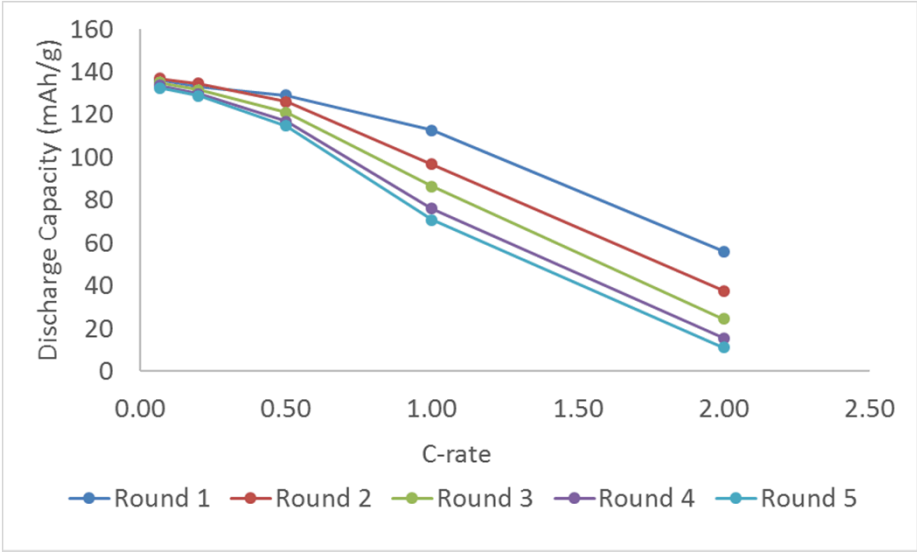

Aging C-rates Tested: C/10, C/5, 1C

Rate Capability

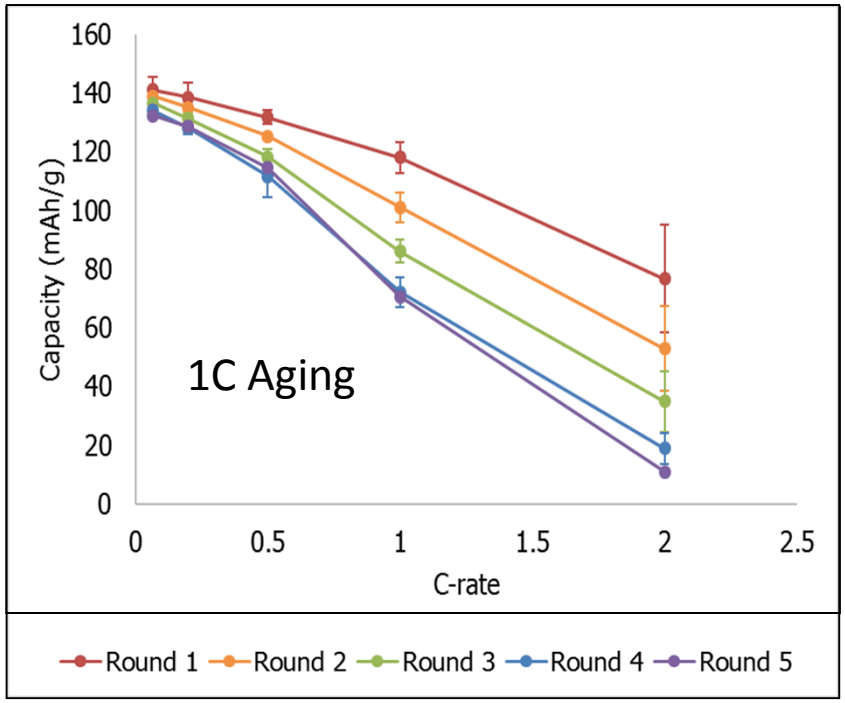

$$Rate\ Capability = \frac{Discharge\ Capacity\ at\ 1C}{Discharge\ Capacity\ at\ C/15}$$

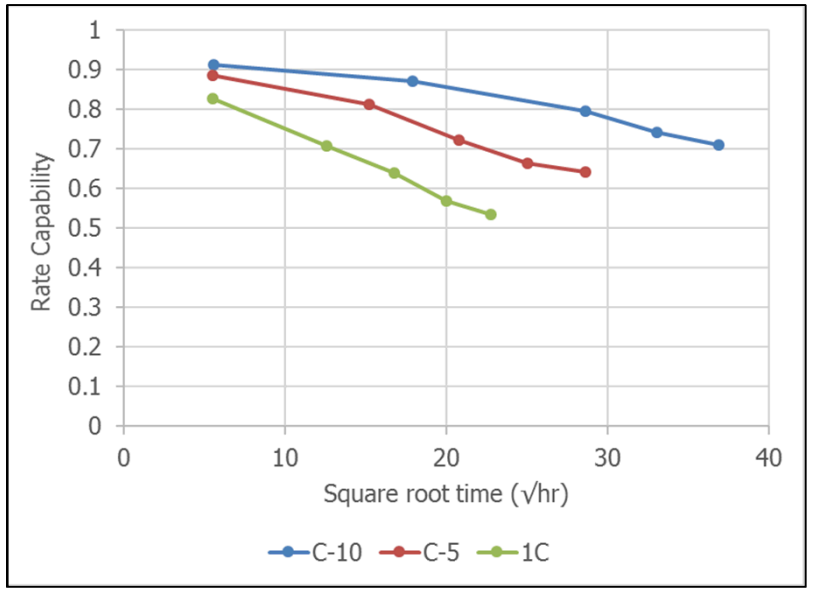

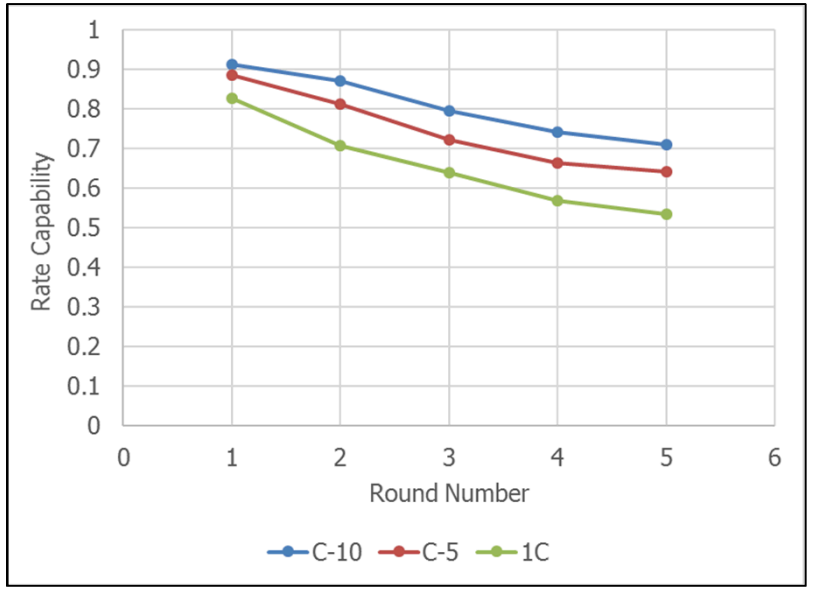

Capacity at C/15

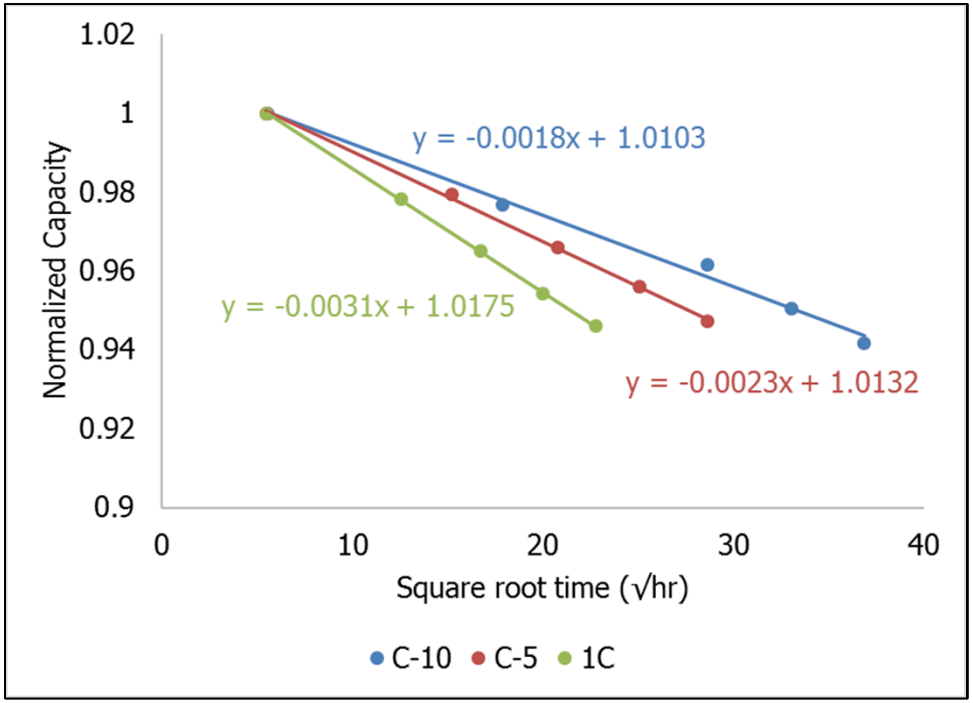

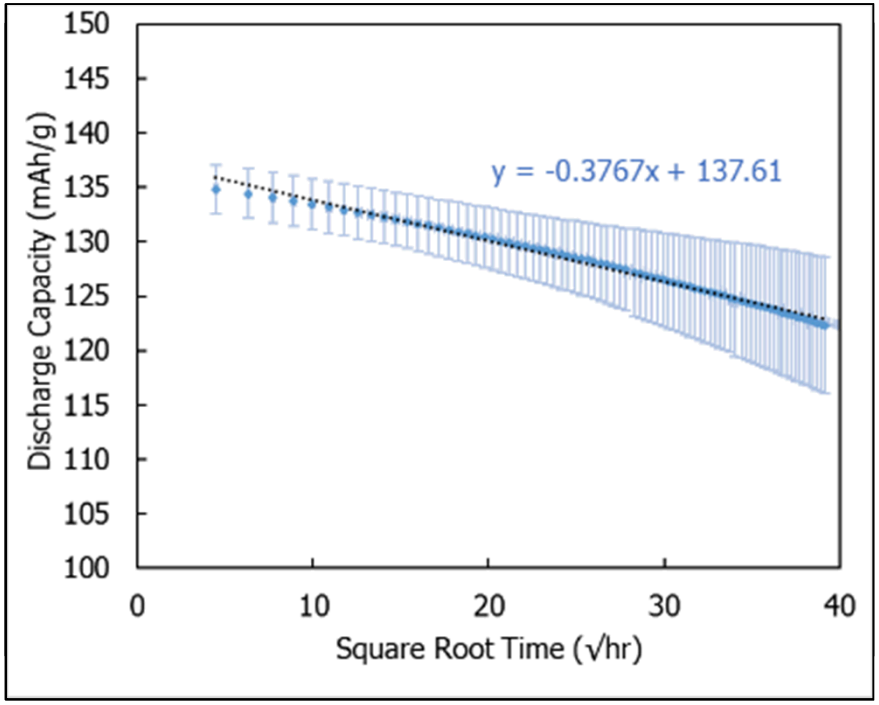

- At C/15 kinetic and polarization effects are minimized and thus we measure a true capacity for the cell
- The loss of capacity agrees with what was seen in long-term testing of cells – Loss of Li inventory through SEI mechanisms
- Therefore, mechanical induced damage has only slight impact on the true capacity for the cell

1C Capacity loss

Square root time

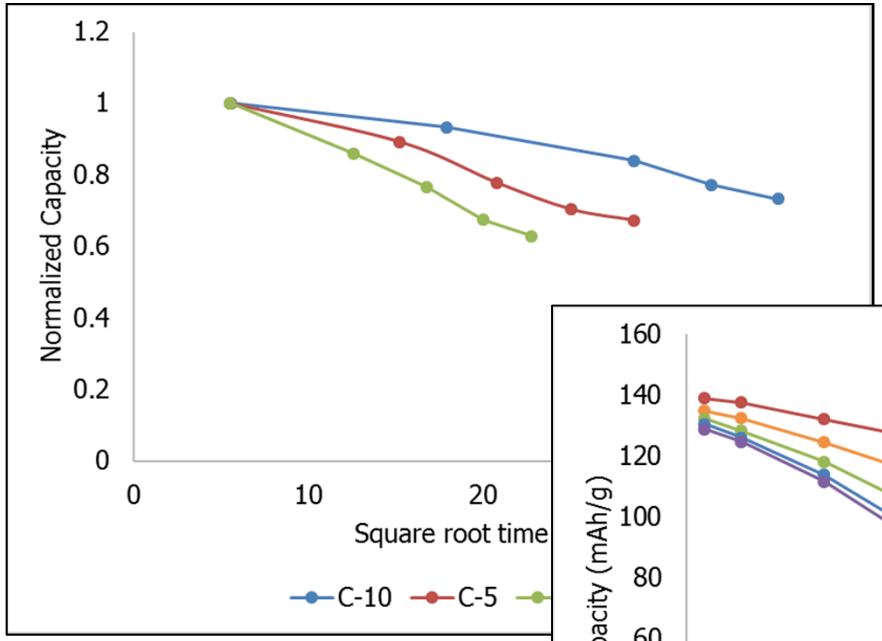

Round Number

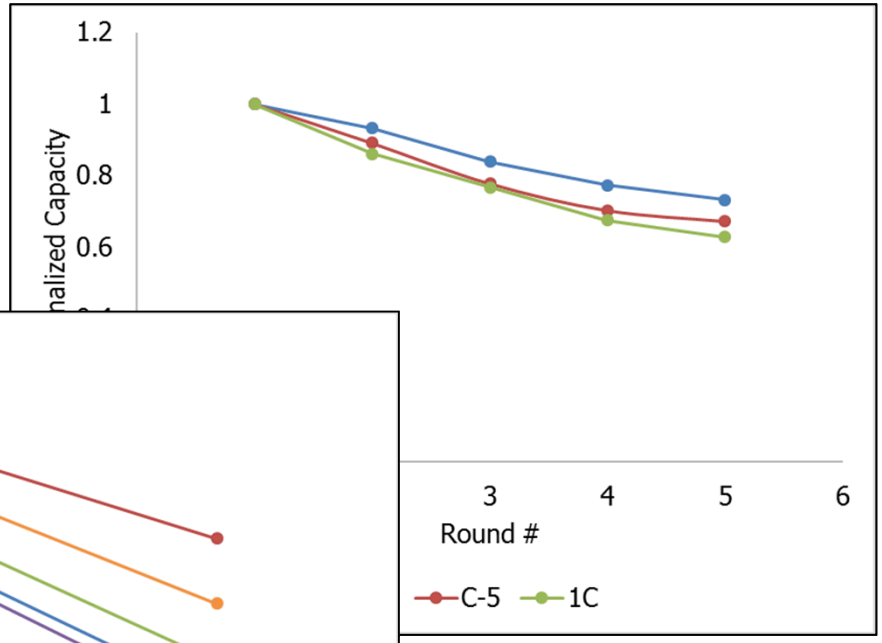

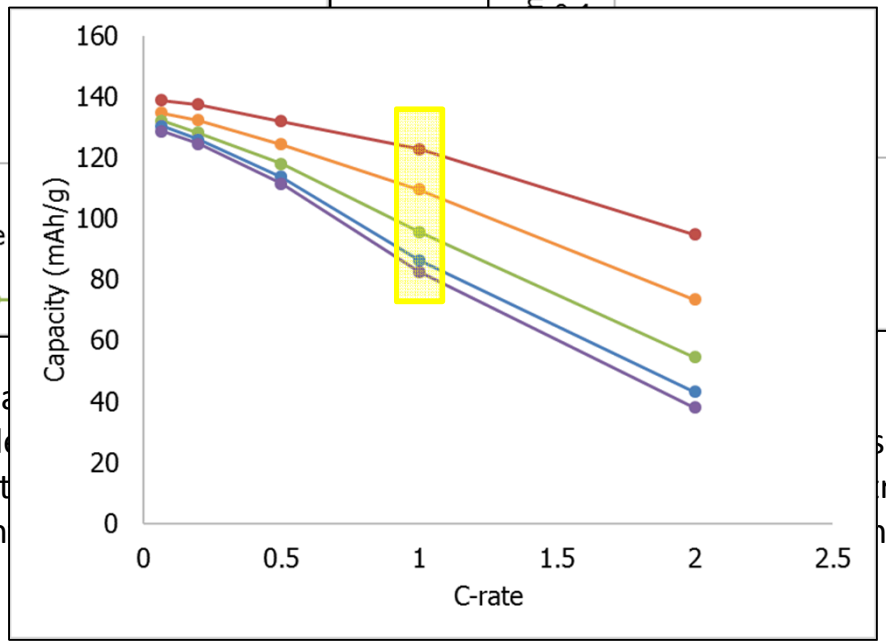

- Chemical mechanisms domina
- In addition to non-recoverabl solation), recoverable mechanisms cont rapping)
- Recoverable mechanisms con h of Li ion through the $LiCoO_2$ particle.

Rate Capability Summary

Slow Rates (C/15)

- Li^+ inventory loss
- Particle isolation

Fast Rates (1C)

- Li^+ inventory loss, surface films
- Particle isolation
- Mechanical-induced degradation (Li ion trapping)

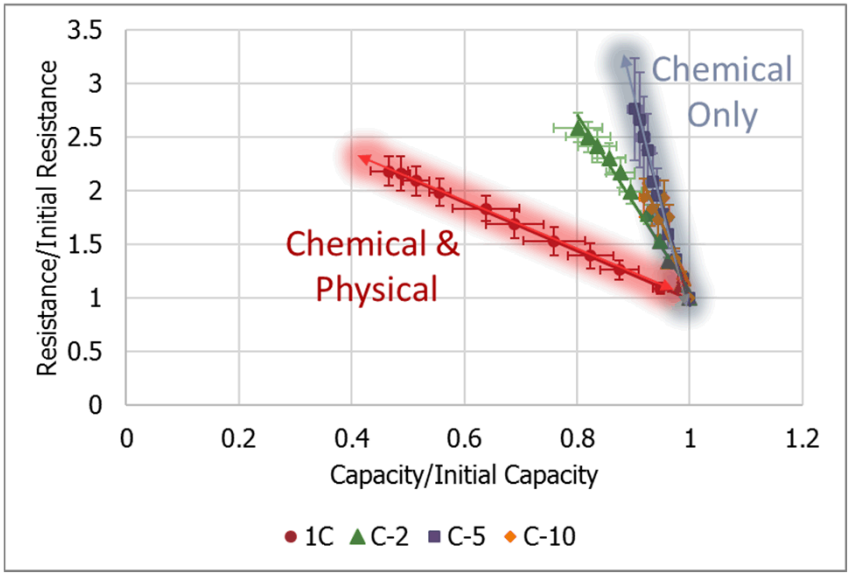

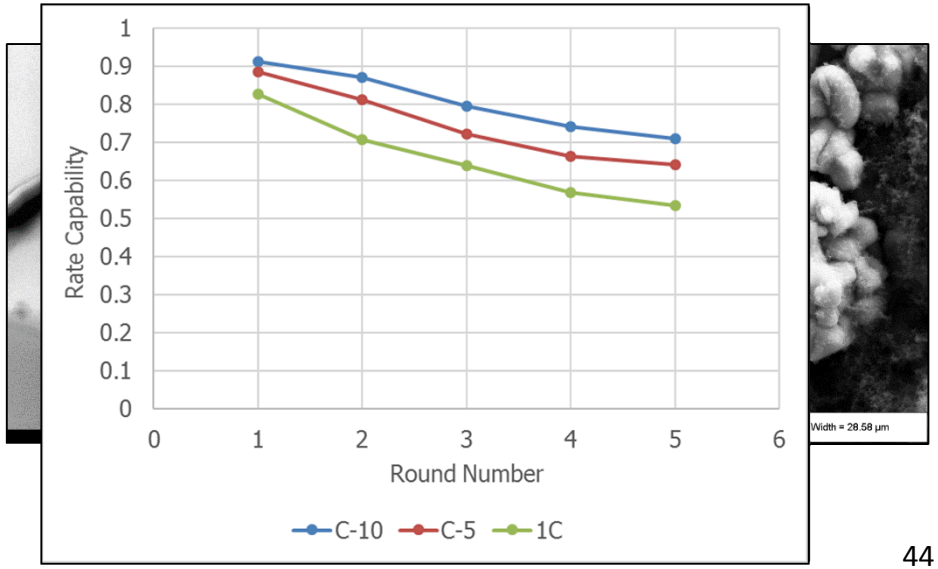

LIB TECHNOLOGY | DEGRADATION | CONCLUSIONS

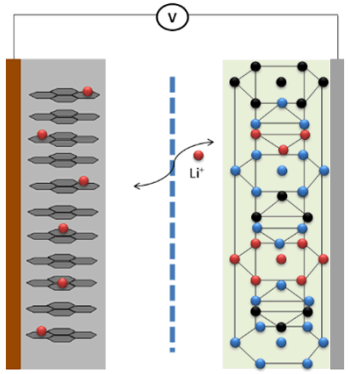

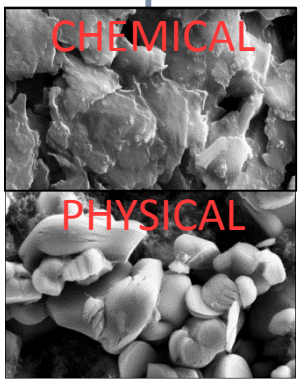

THESIS HYPOTHESIS

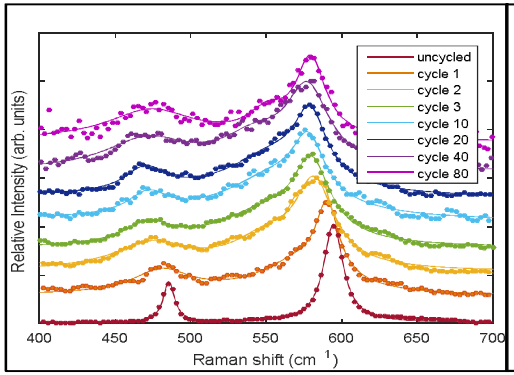

RAMAN SPECTROSCOPY

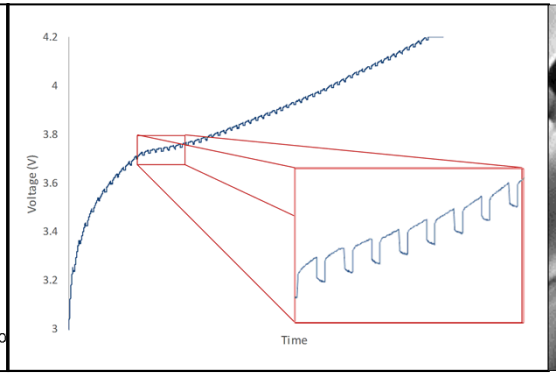

CURRENT INTERRUPT

MICROSCOPY

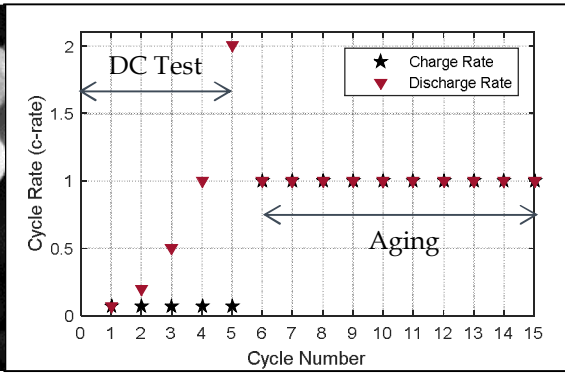

RATE CAPABILITY

Conclusions

- Capacity loss at slow rates (C/10) is exclusively caused by loss of Li inventory through chemical mechanisms of SEI formation and growth.
- For an equivalent amount of chemical degradation, high c-rates result in larger capacity losses attributed to mechanical damage.
- Mechanical damage was most severe in high c-rate electrodes. Damage accumulated in the form of micro-cracks, dislocations, and particle fracture. All of which work to effectively lower solid-state diffusivity of Li^+.
- Rate capability degrades with faster c-rate aging caused by mechanical-induced damage resulting in lowered diffusivity.
- Capacity loss at slow c-rates is attributable to non-recoverable losses in the form of Li inventory loss. Meanwhile, capacity loss at high c-rates combines non-recoverable and recoverable losses where recoverable losses involve limitations from surface films and Li ion trapping.

Final Conclusions

Chemical mechanisms of degradation in a Li-ion battery dominate capacity loss at low c-rates, whereas, mechanical mechanisms dominate at high c-rates.

Takeaways

Creating a more stable SEI and configuring $LiCoO_2$ particle morphology to reduce intercalation stress is critical for improvement of lithium ion batteries.

Chemical mechanisms of degradation in a Li-ion battery dominate capacity loss at low c-rates, whereas, mechanical degradation dominates at high c-rates.

Publications

C. Snyder, C. Apblett, A. Grillet, K. Fenton, D. Duquette "C-rate Effects on Degradation Mechanisms in Li ion cells using Current Interruption Methods "submitting to *Journal of The Electrochemical Society*

C. Snyder, C. Apblett, A. Grillet, D. Duquette "New In-situ Raman Microscopy Coin Cell for Study of Li-ion Electrode Materials" submitting to *Journal of The Electrochemical Society*

C. Snyder, C. Apblett, A. Grillet, T. Beechem, D. Duquette "Measuring Li+ Inventory Losses in $LiCoO_2$/Graphite Cells Using Raman Microscopy" *Journal of The Electrochemical Society* 163 (2016) A1036-A1041

A. Grillet, T. Humplik, E. Stirrup, S. Roberts, D. Barringer, C. Snyder, M. Janvrin, C. Apblett "Conductivity Degradation of Polyvinylidene Fluoride Composite Binder during Cycling: Measurements and Simulations for Lithium-Ion Batteries" *Journal of The Electrochemical Society* 163 (2016) A1859-A1871

Technical Talks

"Measuring Li+ Inventory Losses in $LiCoO_2$/C Cells Using Ex-Situ Raman Spectroscopy", C. Snyder, D. Duquette, C. Apblett, A. Grillet, T. Beechem, 229th Electrochemical Society Meeting, San Diego, CA, May 29-June 3, 2016

"Steps Towards In-situ Studies of the Mechanical Degradation of Lithium Ion Batteries using Fluorescence Confocal Microscopy", C. Snyder, D. Duquette, C. Apblett, A. Grillet, T. Beechem, 227th Electrochemical Society Meeting, Chicago, IL, May 24-28, 2015

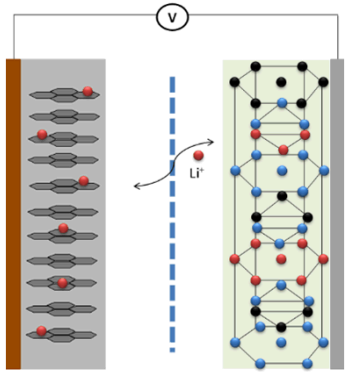

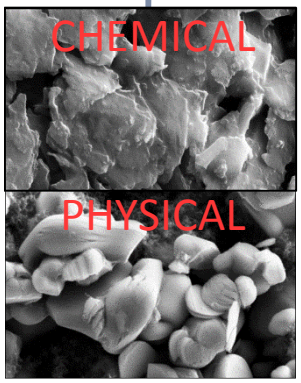

THESIS HYPOTHESIS

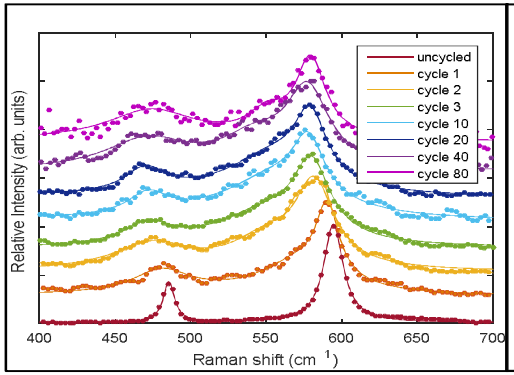

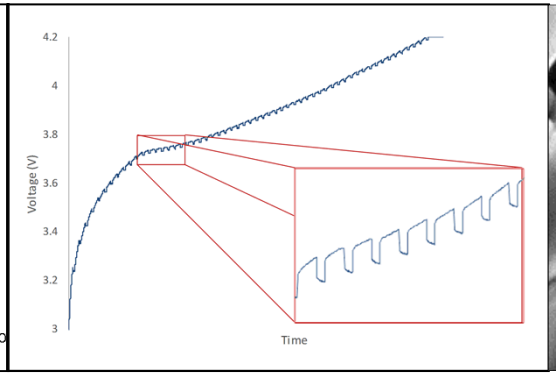

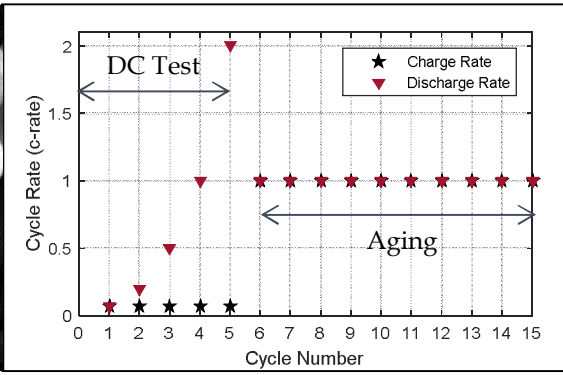

RAMAN SPECTROSCOPY CURRENT INTERRUPT MICROSCOPY RATE CAPABILITY

Acknowledgements

- **Thesis Advisors**: Professor David Duquette, Dr. Christopher Apblett
- **Sandia Advisor**: Dr. Anne Grillet
- **Committee Members**: Professor Vidya Chakrapani, Professor Daniel Lewis, Professor Linda Schadler, and Dr. Daniel Wesolowski
- **Group Members**: Dr. Brian Perdue, Dr. Jonathan Coleman, Hannah Height, Josey McBrayer, Jaclyn Coyle

Sandia Acknowledgements

Gail Baca
Dr. Thomas Beechem
Dr. Victor Brunini
Lorie Davis
Dr. Farid El Gabaly
Dr. Kyle Fenton
Dr. Paul Kotula
Jessica Kruichak
Lisa Lowery
Anthony McDonald
Bonnie Mckenzie
Dr. Mani Nagasubramanian
Dr. Christopher Orendorff
Dr. Harry Pratt
Cherisse Rigby
Dr. Scott Roberts
Dr. Jeremy Walraven

Thank you
Questions?

List of Backup Slides

1. Raman Power – Heat Generated
2. Raman Study at 1C
3. SEI with square root time references and data
4. Estimating SEI thickness with square root time by capacity loss
5. Detecting SEI
6. CC vs CCCV Mode
7. Compare Cells to Commercial Cells
8. EIS Data – why use CI as opposed to EIS?
9. Li Diffusion mechanism
10. RCI Measurements
11. Microtome Results
12. Non-recoverable capacity loss from high c-rate cycling
13. Rate Capability comparison to literature values
14. Uncycled Resistance Rise
15. Weppner Assumptions

2. Raman Study at 1C

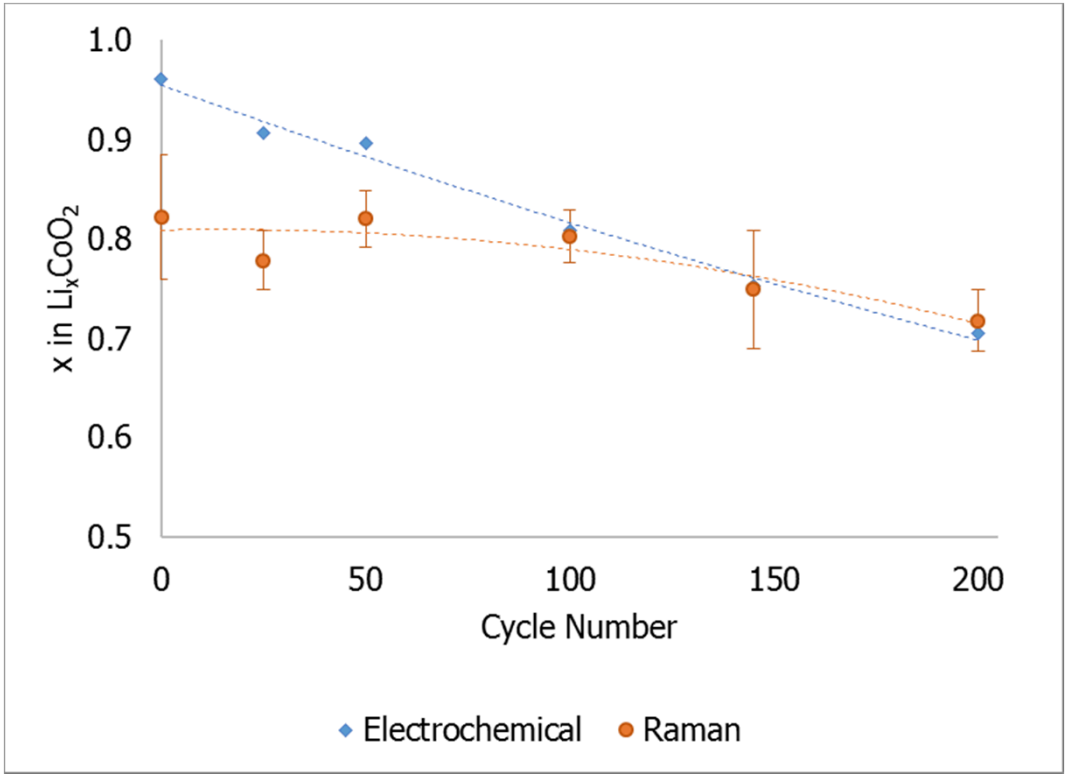

3. Estimating SEI thickness with square root time by capacity loss

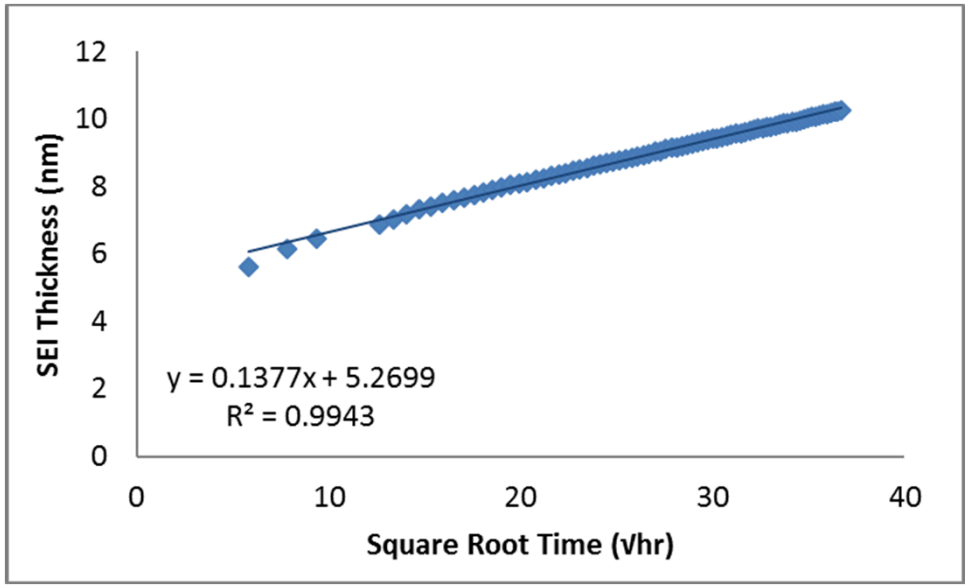

Estimated using methods described by:
G. Zhuang et al *J. Phys. Chem. B.* 109 (2005) 17567-17573

EC Decomposition into lithium ethylene dicarbonate $(CH_2OCO_2Li)_2$

$$2EC + 2\,e^- + 2Li \rightarrow (CH_2OCO_2Li)_2 + CH_2 = CH_2$$

One Monolayer
3Å thick

A.J. Smith et al. *J. Electrochem. Soc.* 158 (2011) A447-A452
A. Colclasure et al. *Electrochimica Acta* 58 (2011) 33-43

5. Detecting SEI

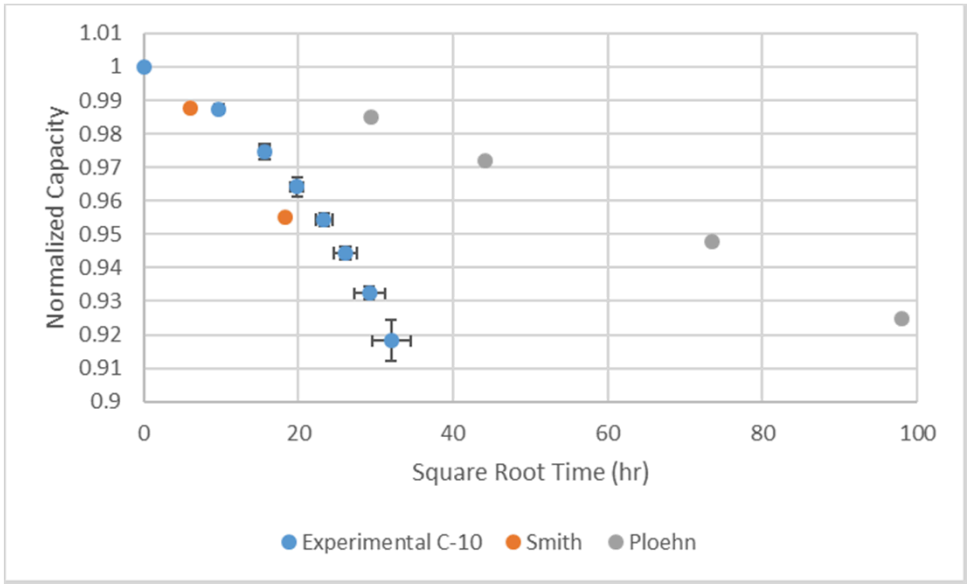

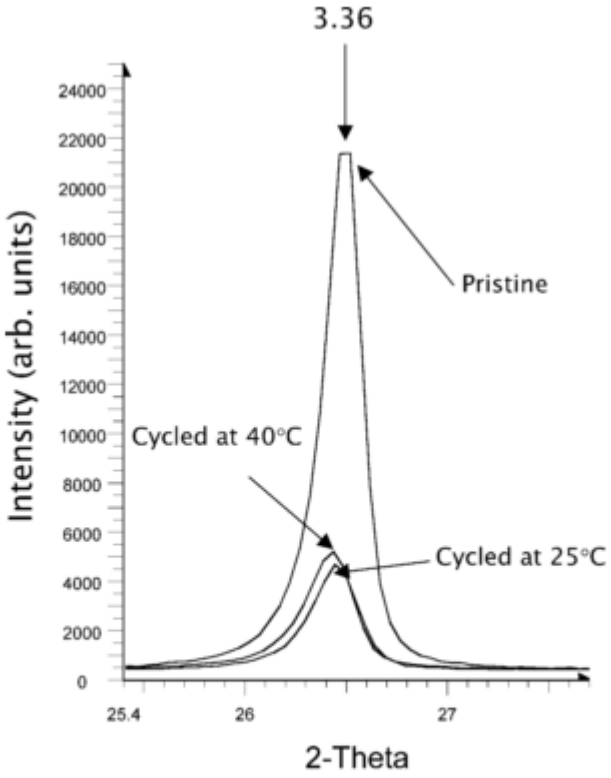

Fig. 9. XRD patterns measured from a pristine anode (on a copper-foil current collector) and XRD patterns measured from anodes after prolonged cycling of 18650-type batteries at 25 and 40 °C, as indicated.

D. Aurbach et al. / Electrochimica Acta 00 (2002) 1–13

6. CC vs CCCV Mode

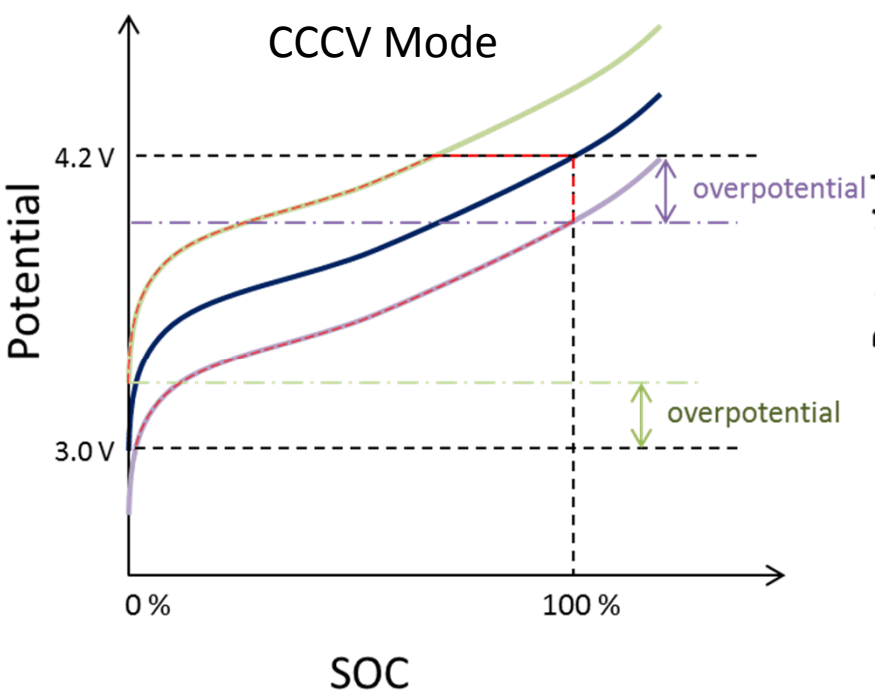

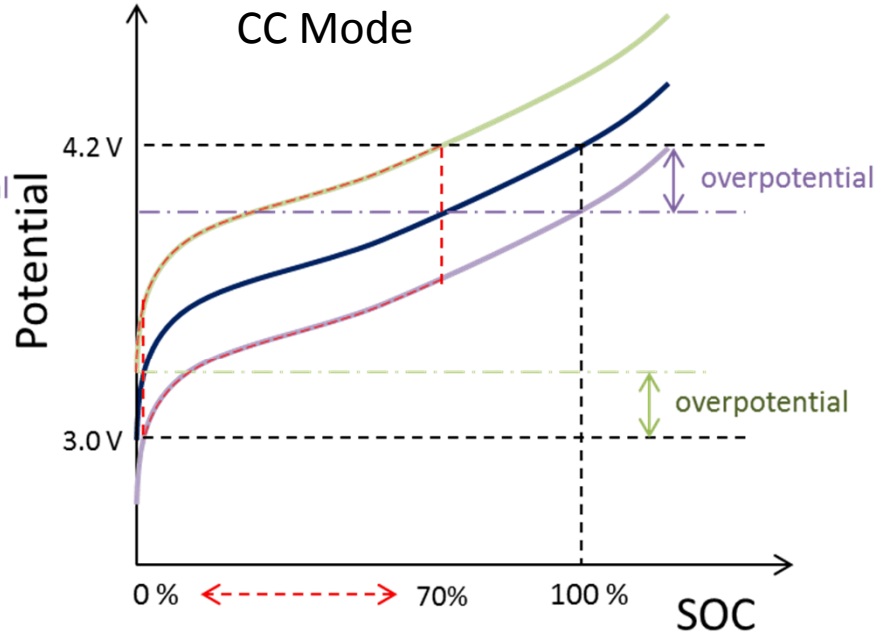

7. Commercial vs Research Grade Cells

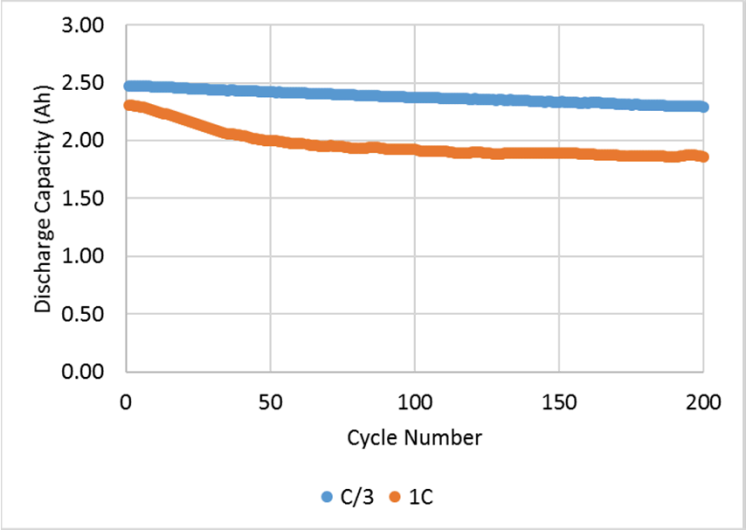

Discharge capacity with cycle number for commercial cell (LG ICR18650C2) cycled at 1C and C/3 rate.

Discuss Cathodes

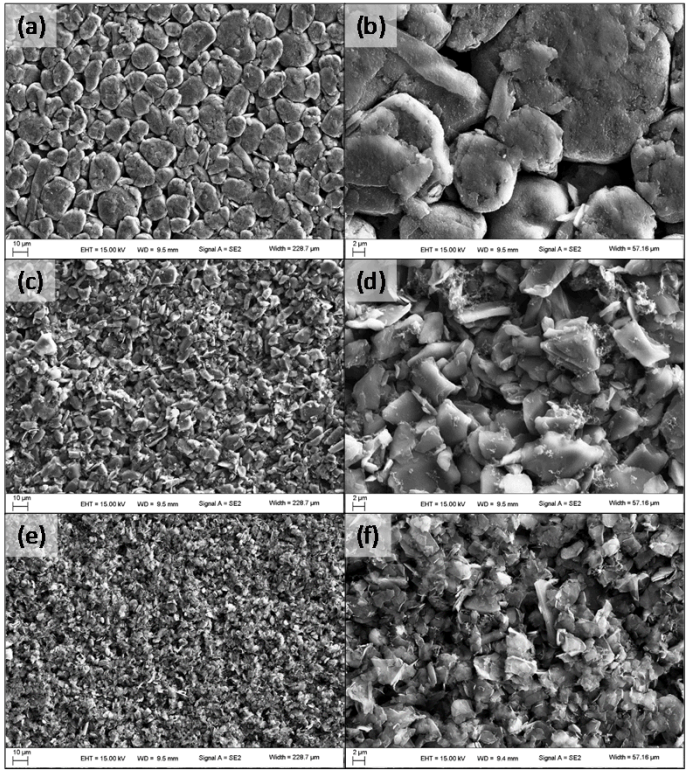

SEM images of (a,b) commercial (LG ICR18650C2), (c,d) G8 research grade, and (e,f) KS-6 research grade graphite anodes. Images in left column are of same magnification and images in right column are of same magnification.

8. EIS Data

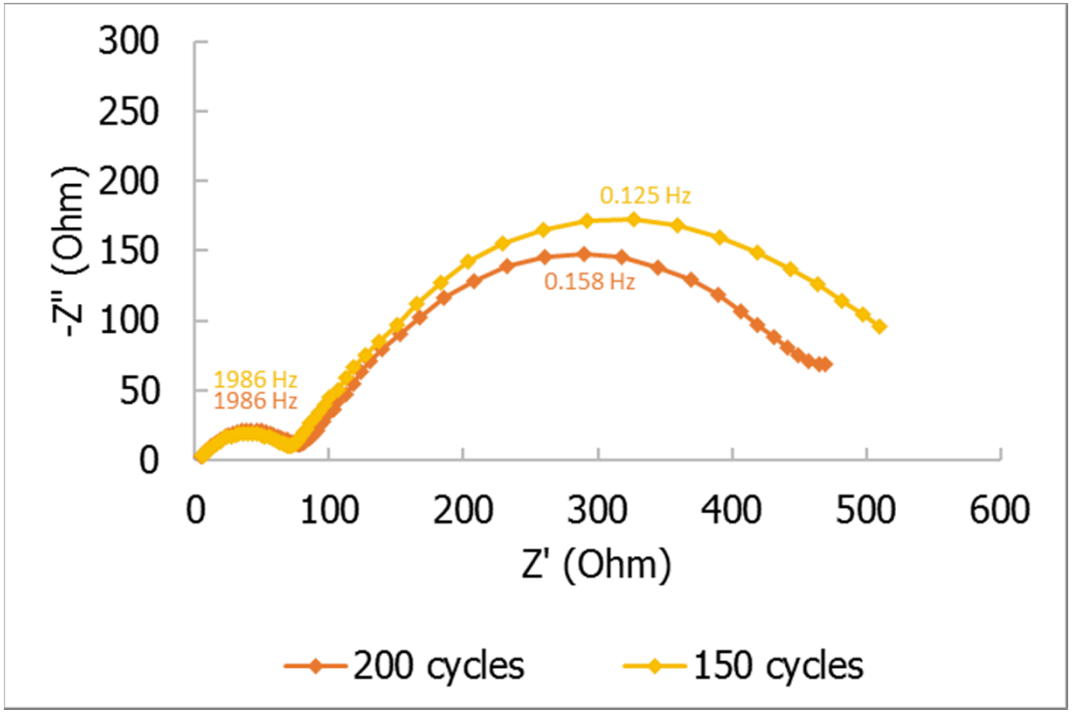
300
250
200
150
100
50
0
-Z'' (Ohm)
0.125 Hz
0.158 Hz
1986 Hz
1986 Hz
0
100
200
300
400
500
600
Z' (Ohm)
200 cycles
150 cycles

9. Li Mechanism

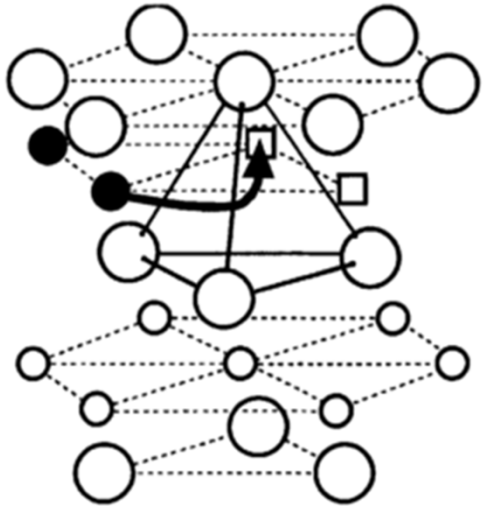

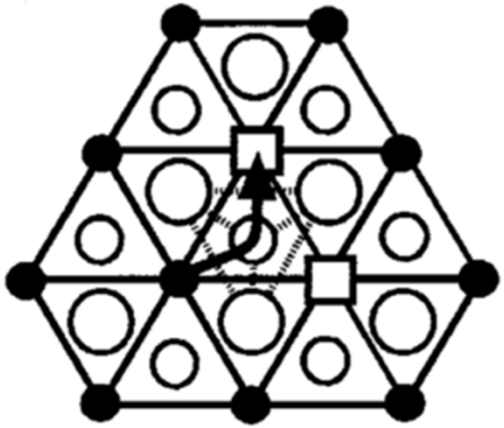

A. Van der Ven and G. Ceder, *J. Power Sources*, 97-8 529-531 (2001)
A. Van der Ven and G. Ceder, *Electrochem. Solid State Lett.*, 3 (7), 301-304 (2000)

10. RCI Measurements

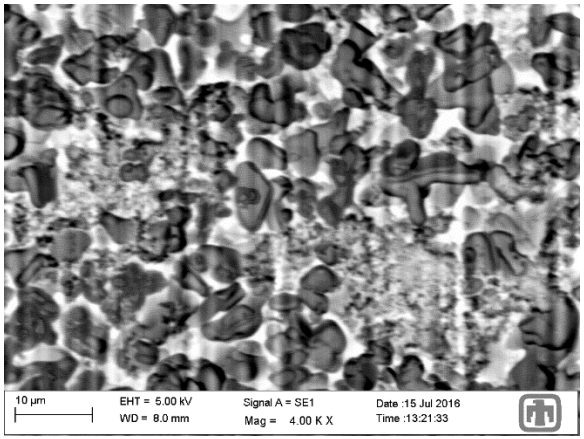

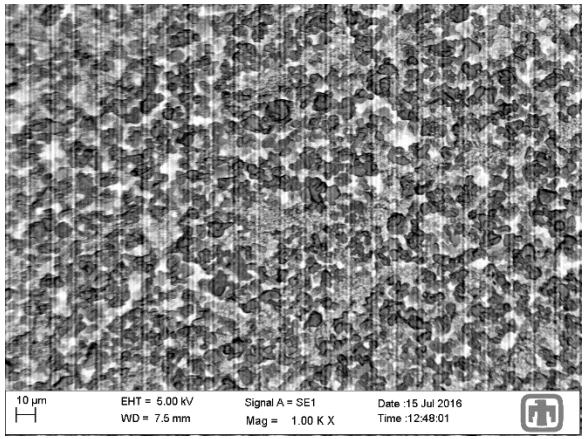

Uncycled

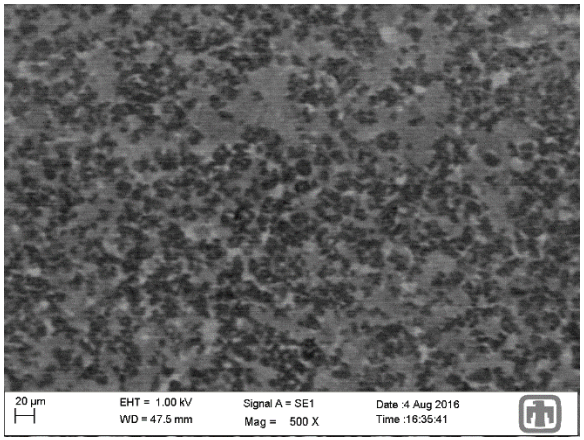

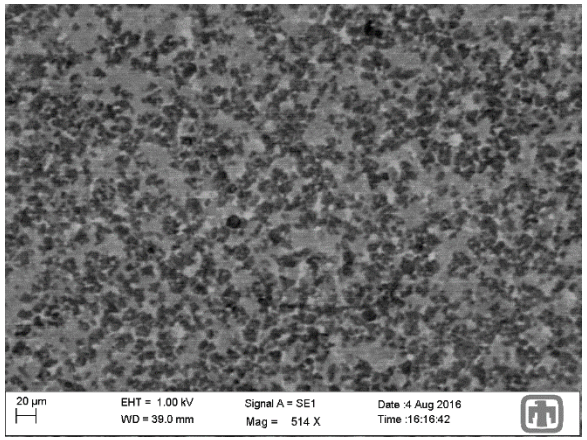

1C 100 cycles

11. Microtome Results

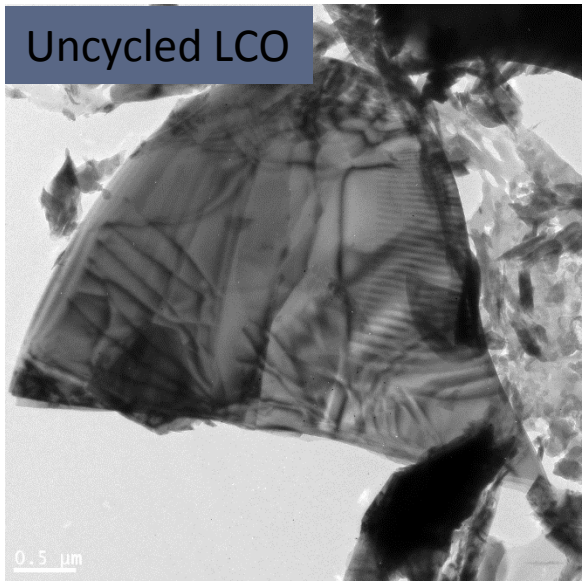

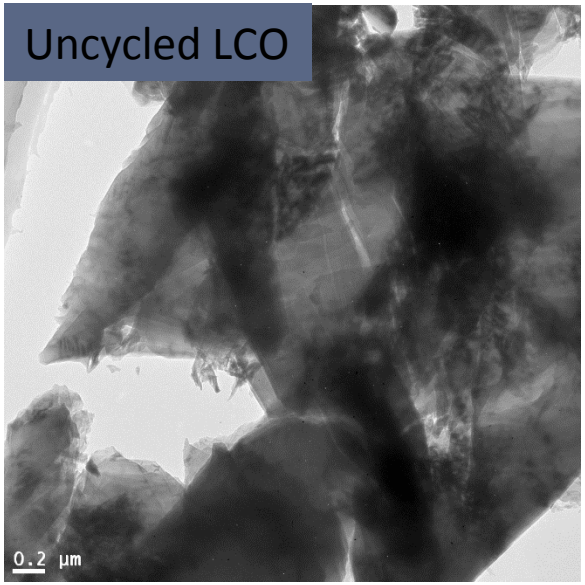

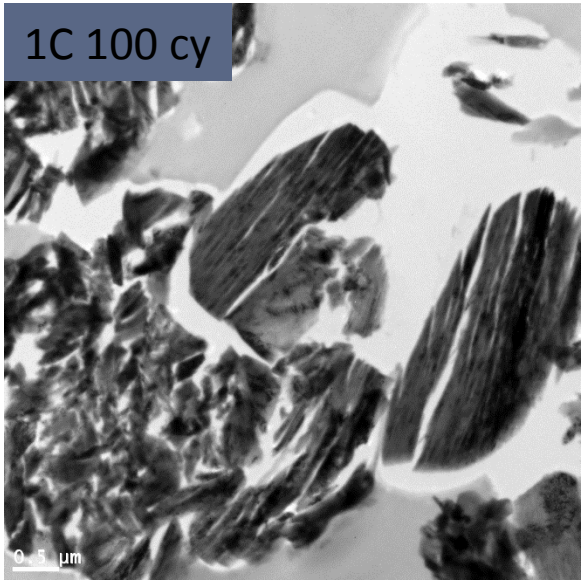

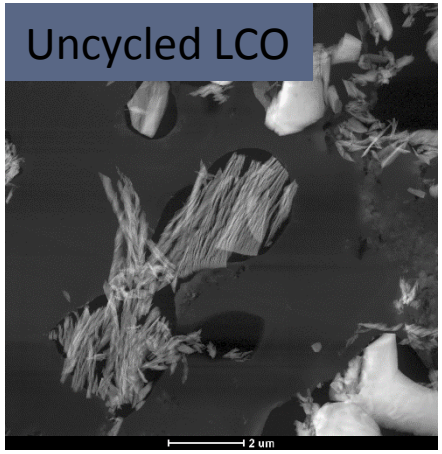

12. Non-recoverable capacity loss from high c-rate cycling

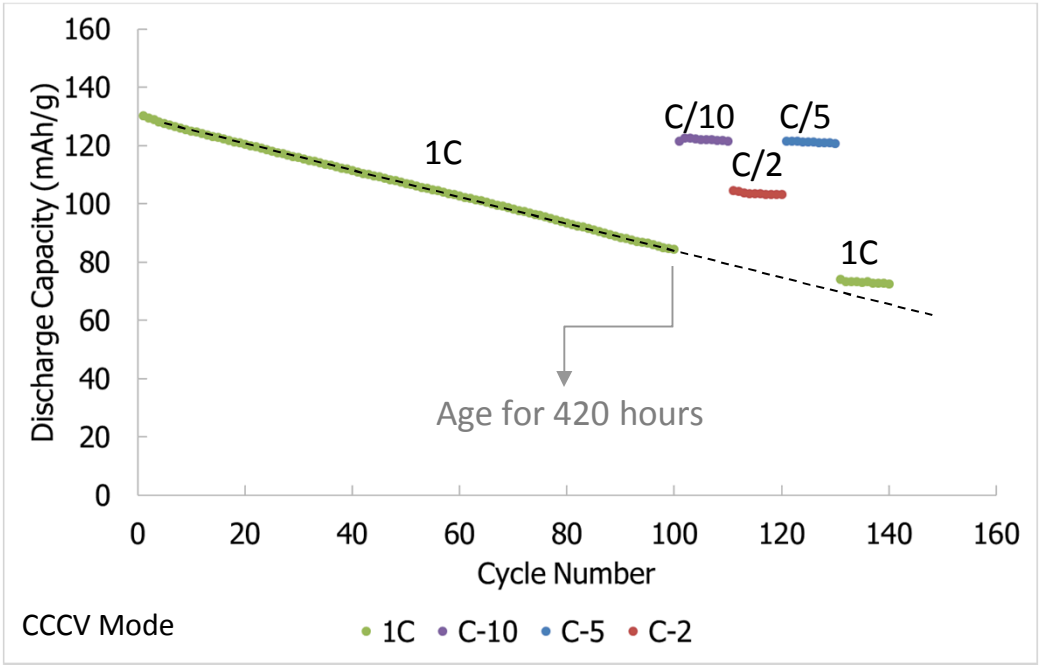

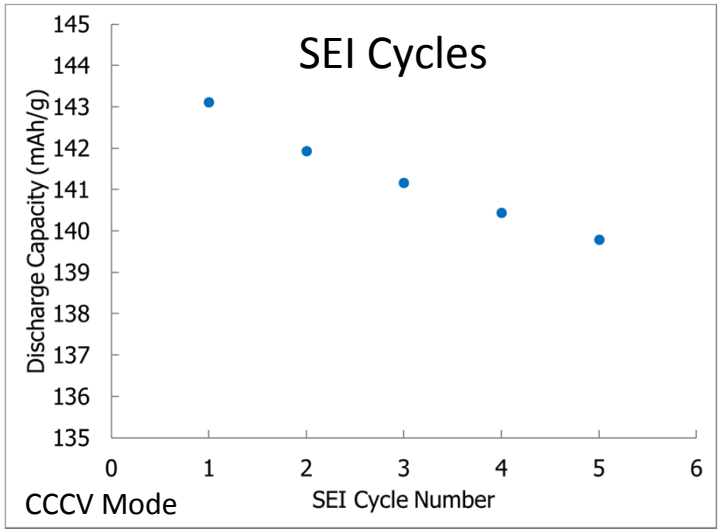

Capacity loss after 824 hours as measured at C/10

C/10 Cycling: $5.8 \pm 0.2\%$
1C Cycling: 13.0%

13. Rate Capability

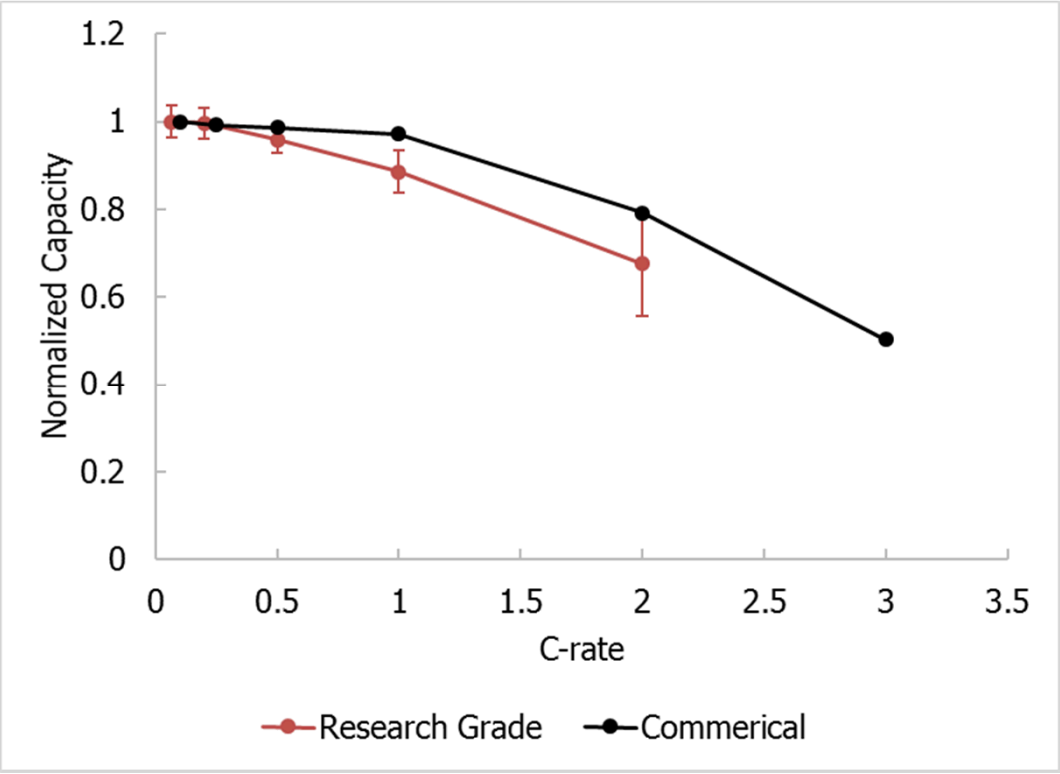

14. Uncycled Resistance Rise

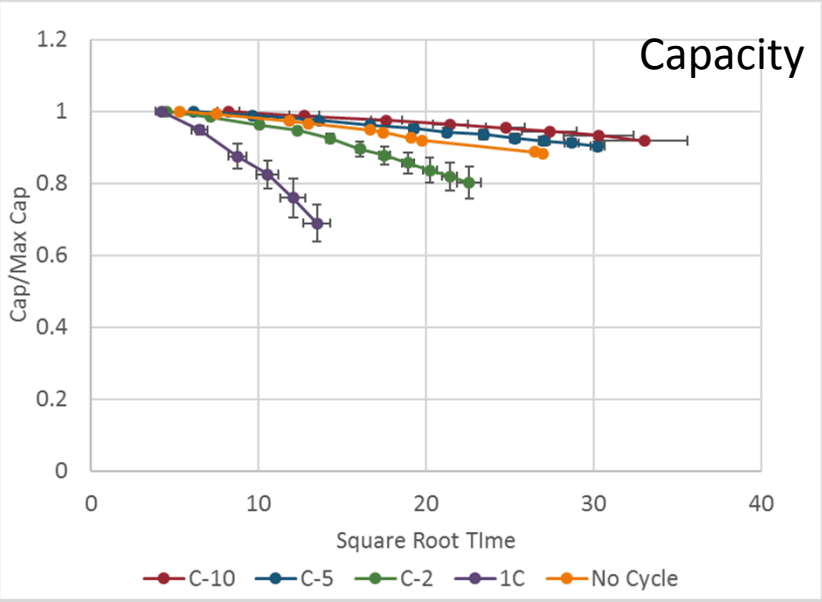

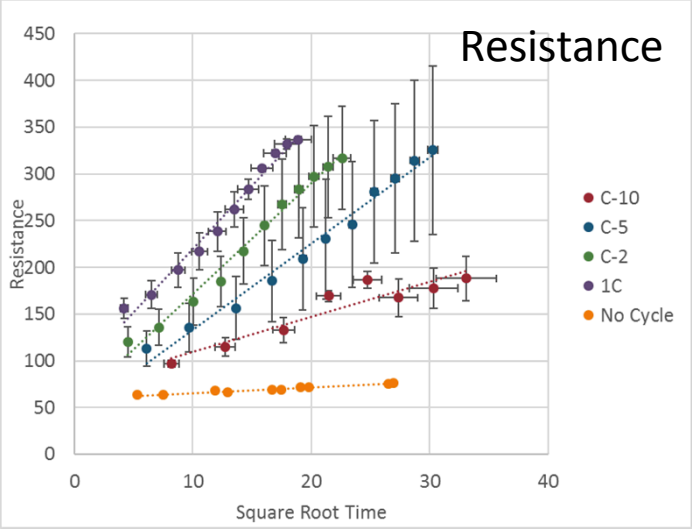

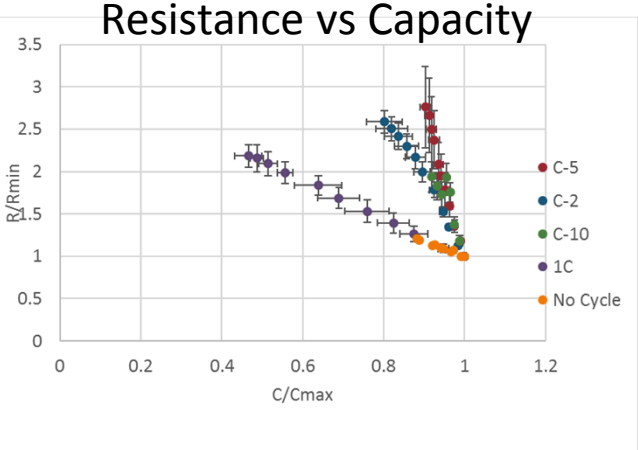

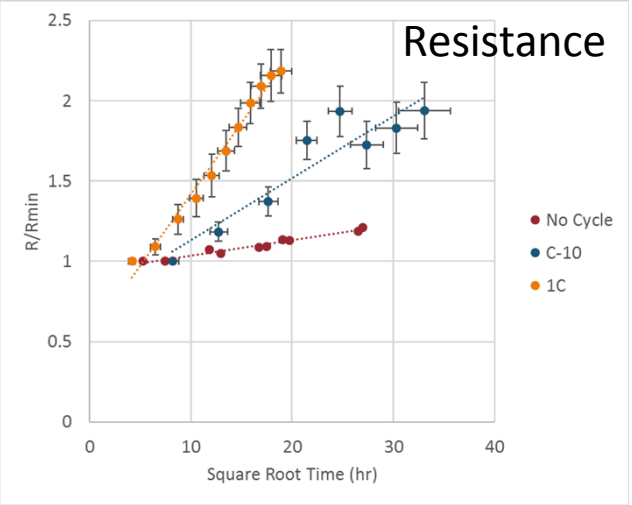

Surface Films on $LiCoO_2$ Cathode

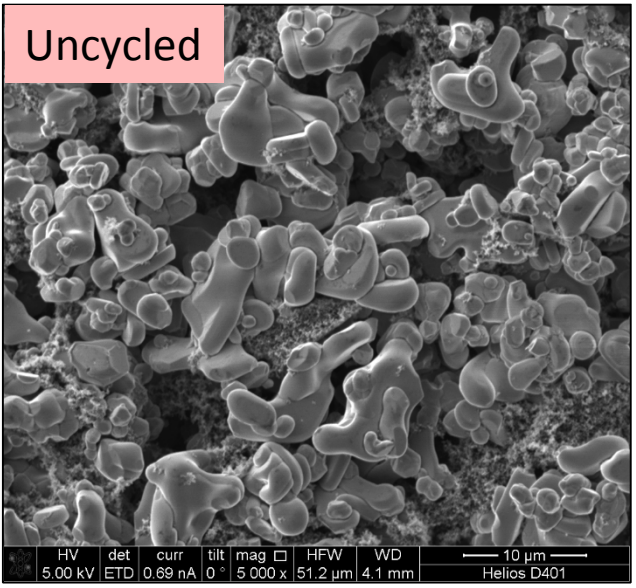

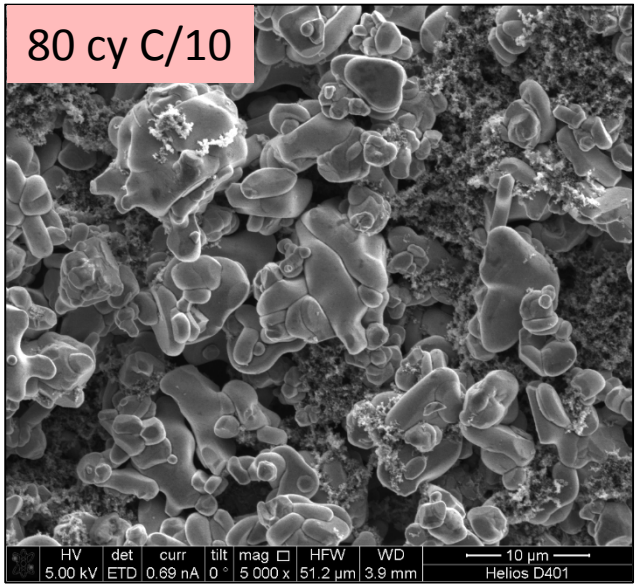

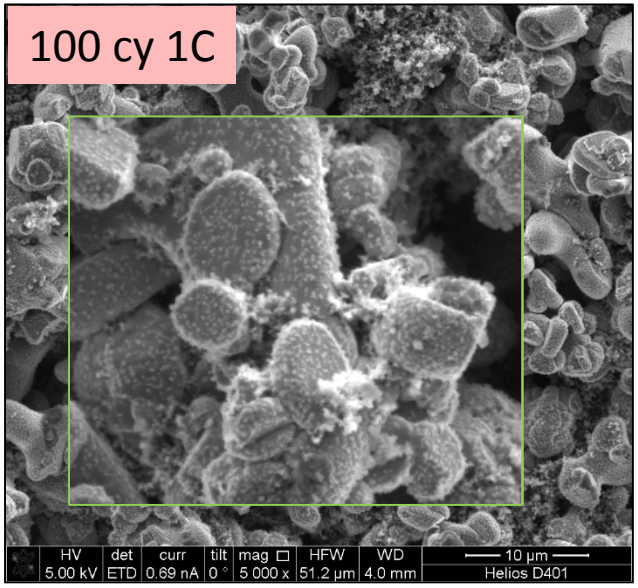

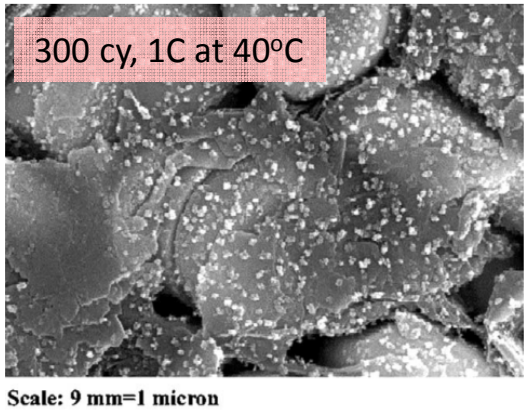

Larger polarizations, more time spent at 4.2V during CCCV mode

D. Aurbach et al. *Electrochimica Acta* 47 (2002) 1899-1911

Questions to Prep for

- Impedance vs Resistance
- LiCoO2 synthesis process
- How would u measure dislocation density?
- What type of defects can you get in a ionic crystal – dislocations, frenkl and schottky point defects – charge neutraility
- Active glide plane? Cleavage plan in crystal structure?
- FIB Process

Conclusions

- **Coin Cell Testing:** High c-rates accelerate capacity loss
- **Raman Microscopy:** Capacity loss at slow rates (C/10) is exclusively caused by loss of Li inventory through chemical mechanisms of SEI formation and growth.
- **Current Interrupt:** For an equivalent amount of chemical degradation, high c-rates result in larger capacity losses attributed to mechanical damage
- **Microscopy:** Mechanical damage was most severe in high c-rate electrodes. Damage accumulated in the form of micro-cracks, dislocations, and particle fracture. All of which work to effectively lower solid-state diffusivity of Li^+.
- **Rate Capability**: Rate capability degrades with faster c-rate aging caused by mechanical-induced damage resulting in lowered diffusivity. Capacity loss at slow c-rates is attributable to non-recoverable losses in the form of Li inventory loss. Meanwhile, capacity loss at high c-rates combines non-recoverable and recoverable losses where recoverable losses involve limitations from surface films and Li ion trapping.

Final Conclusions

Chemical mechanisms of degradation in a Li-ion battery dominate capacity loss at low c-rates, whereas, mechanical mechanisms dominate at high c-rates.

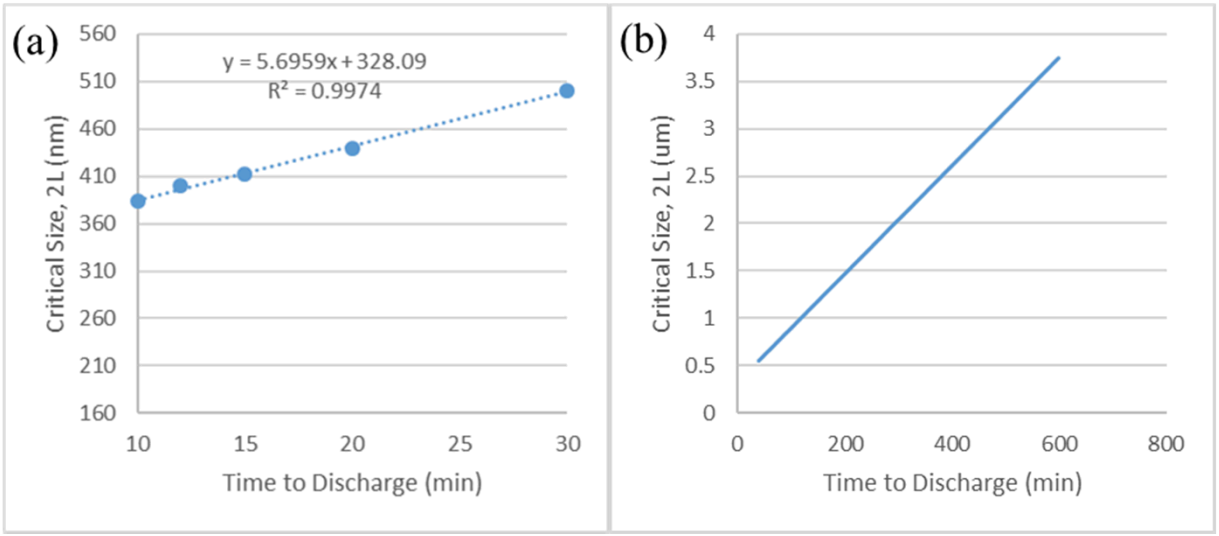
(a)
y = 5.6959x + 328.09
R² = 0.9974
Critical Size, 2 L (nm)
560
510
460
410
360
310
260
210
160
10
15
20
25
30
Time to Discharge (min)
(b)
Critical Size, 2 L (um)
4
3.5
3
2.5
2
1.5
1
0.5
0
0
200
400
600
800
Time to Discharge (min)